Band structure

-> ARUPS (ARPES)

Chemical composition

-> XPS, Auger

## **Spectroscopy**

Magnetism

-> XAS, XMCD

Bond orientation

-> XLD

Structure modification

-> EXAFS

• • •

• • •

. . .

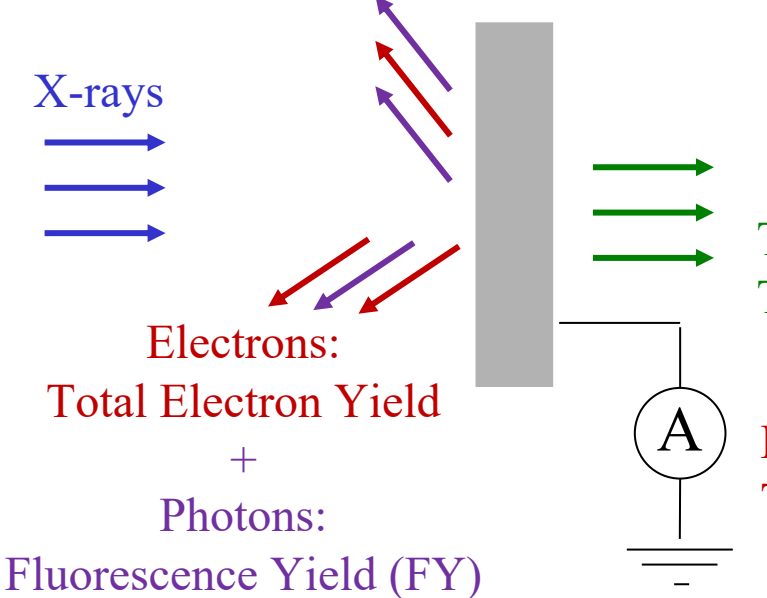
#### XAS vs. XPS

#### XAS:

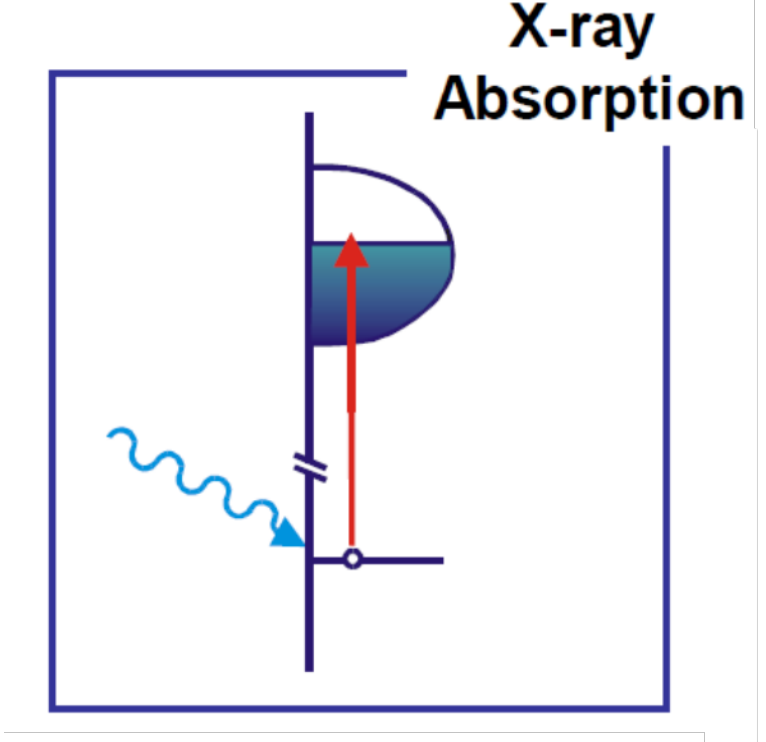
incoming phonons with **tuned energy**.

Maximum absorption for resonant excitation from a core level to a valence state

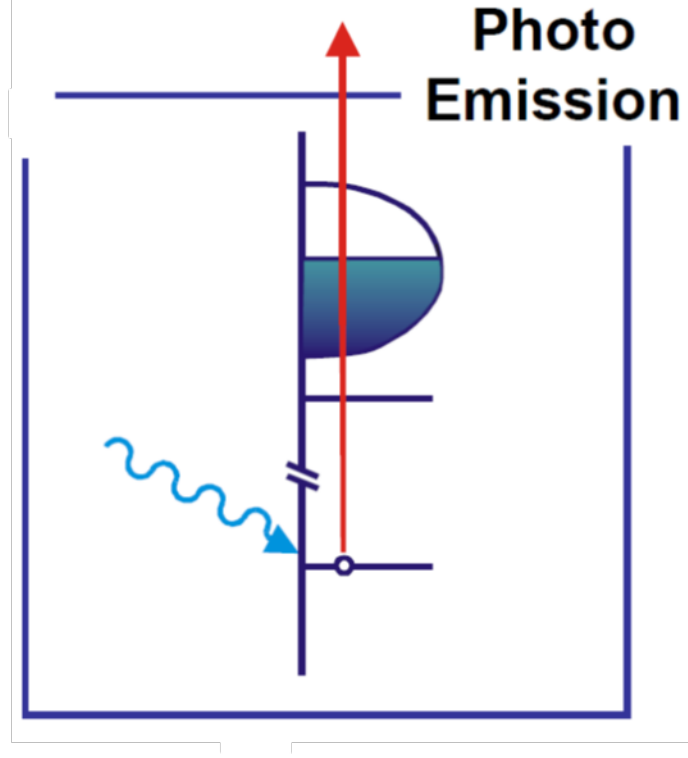
XAS detection scheme determines the depth sensitivity



XAS
X-ray absorption spectroscopy



XPS
X-ray photoelectron spectroscopy



Transmitted X-rays:

Transmission Yield (TY)

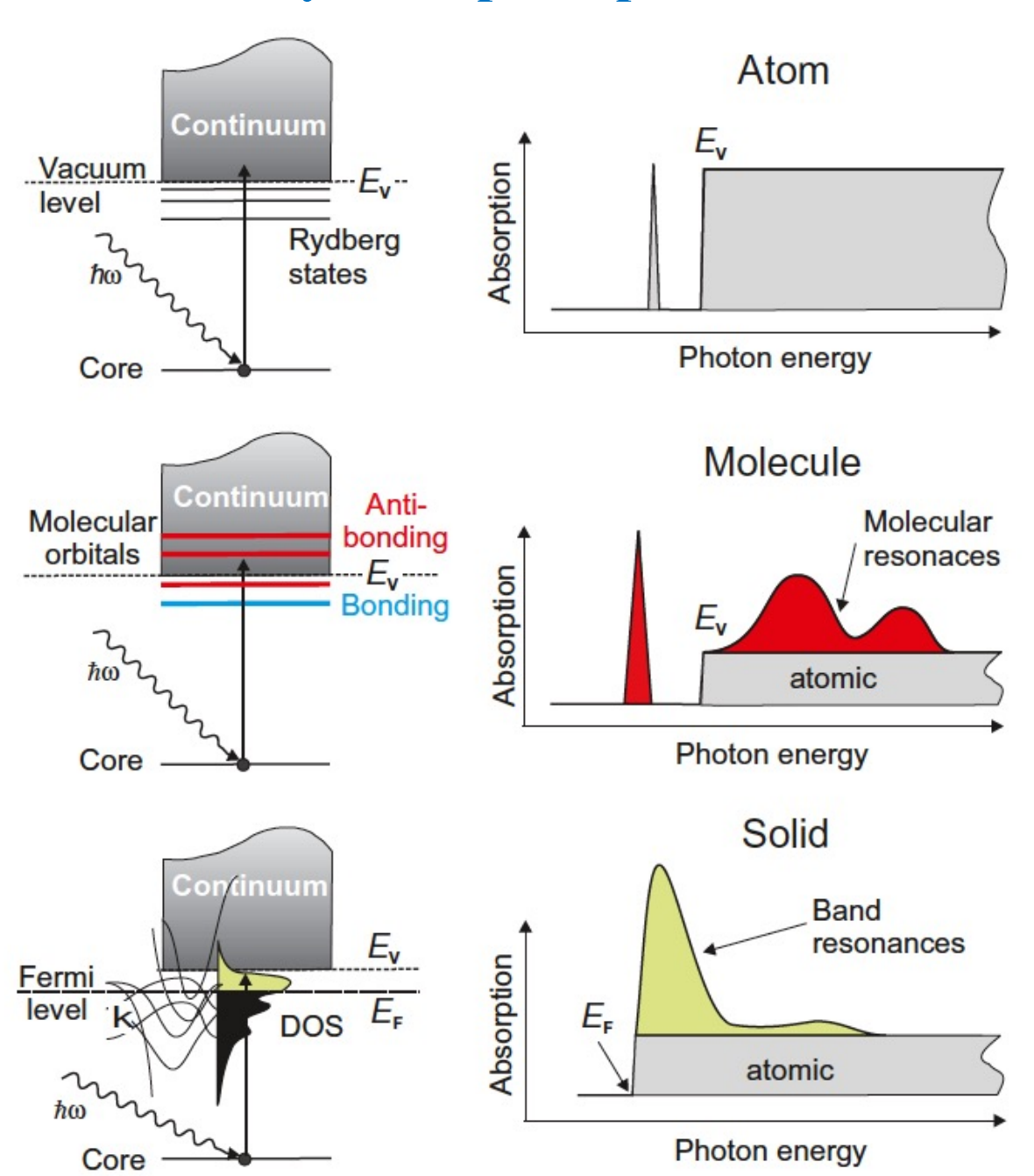
Measure of the emitted electrons: Total Electron Yield (TEY)  $TEY \longrightarrow$ 

→ surface sensitive

TY, FY

→ bulk sensitive

## X-ray absorption process



## X-ray absorption process

The transition probability per unit time from an initial state *i* to a final state f

$$w_{i\to f} = \frac{2\pi}{\hbar} |\langle f | \mathcal{H}_{int} | i \rangle|^2 \delta(\varepsilon_f - \varepsilon_i - \hbar\omega)$$

x-ray absorption intensity per atom, electron dipole approximation

$$I = 4\pi^2 \frac{e^2}{\hbar c} \hbar \omega |\langle f | \hat{\mathcal{E}} \cdot \mathbf{r} | i \rangle|^2$$

 $P_q^{(1)} = \hat{\mathcal{E}}_q \cdot \mathbf{r}$  dipole operator, q polarization

 $\hbar\omega$  energy required to excite the electron from initial to final state

$$\hat{\mathcal{E}}_{q=\pm 1} = \mp \frac{1}{\sqrt{2}} (\hat{\mathbf{e}}_x \pm i\hat{\mathbf{e}}_y)$$

 $\overline{\mathcal{E}}$  unit electric field vector

$$\hat{\mathcal{E}}_{q=0} = \hat{\mathbf{e}}_z$$

 $\mathbf{r} = x\hat{\mathbf{e}}_x + y\hat{\mathbf{e}}_y + z\hat{\mathbf{e}}_z$  electron position

Racah's operators

$$P_{\pm 1}^{(1)} = \mp \frac{1}{\sqrt{2}} (x \pm iy) = rC_{\pm 1}^{(1)} = r\sqrt{\frac{4\pi}{3}} Y_{1,\pm 1}$$

right and left circular polarization (photon spin  $q = \pm 1$ )

$$P_0^{(1)} = z \qquad \qquad = rC_0^{(1)} = r\sqrt{\frac{4\pi}{3}}Y_{1,0} \qquad \text{linear polarization (photon spin } q=0)$$

#### X-ray absorption process

focussing on the angular part of the electronic states, we see that the matrix elements consist of integrals involving the product of spherical harmonics

$$|\langle f|rC_q^{(1)}|i\rangle|^2$$

example: 
$$\left| \int \int \sin \vartheta \, \mathrm{d}\vartheta \, \mathrm{d}\phi \, Y_{2,2}^* \sqrt{\frac{4\pi}{3}} Y_{1,1} \frac{1}{\sqrt{3}} Y_{1,0} \right|^2$$
 final state operator initial state



## dipole selection rules

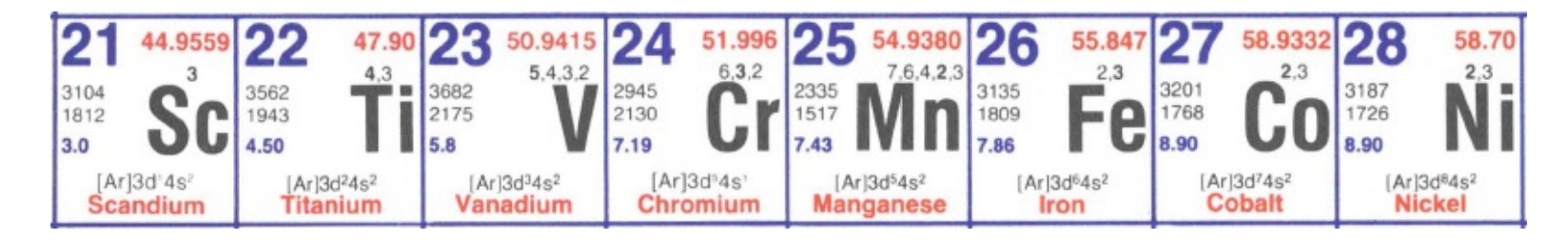
$$\Delta l = \pm 1$$

$$\Delta l = \pm 1$$
 $\Delta m_l = 0, \pm 1$ 
 $\Delta s = 0$ 
 $\Delta m_s = 0$ 

$$\Delta m_s = 0$$

related to polarization

## XAS: example of $L_2$ , $L_3$ edges

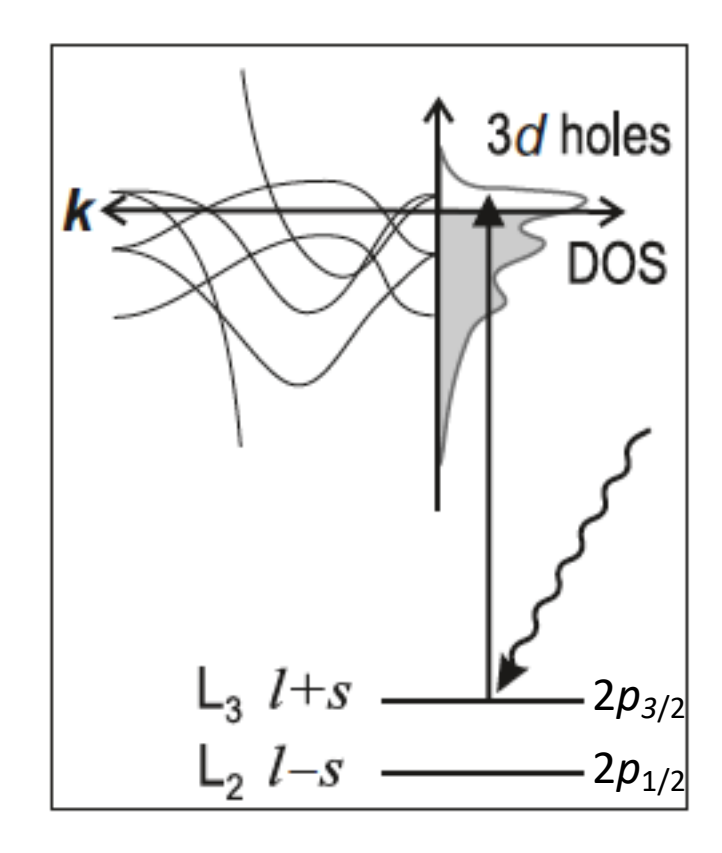


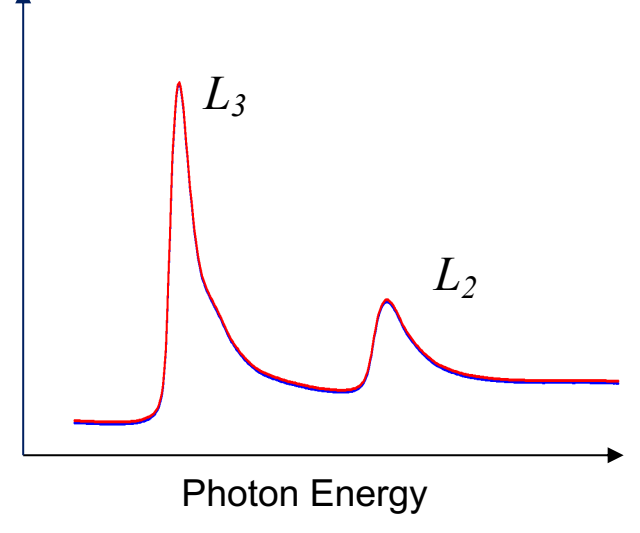
2p levels (6 electrons) each electrons has l=1, and s=1/2total angular momentum for each electron: j = l+s, ...  $|l-s| \rightarrow j=3/2$ , 1/2The basis describing the states is  $|l, s, j, m_j>$ 

Due to spin-orbit coupling, the states with j = 1/2 (L<sub>2</sub> edge) have a different energy than the ones with j = 3/2 (L<sub>3</sub> edge)

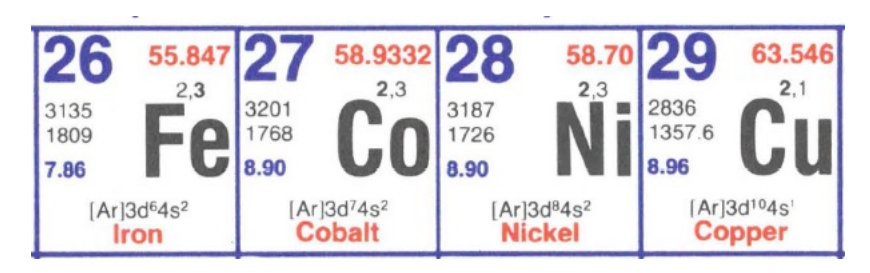
The antiparallel configuration  $(2p_{1/2})$  is energetically favorable, i.e. has higher binding energy, therefore it requires higher photon energy to be reached

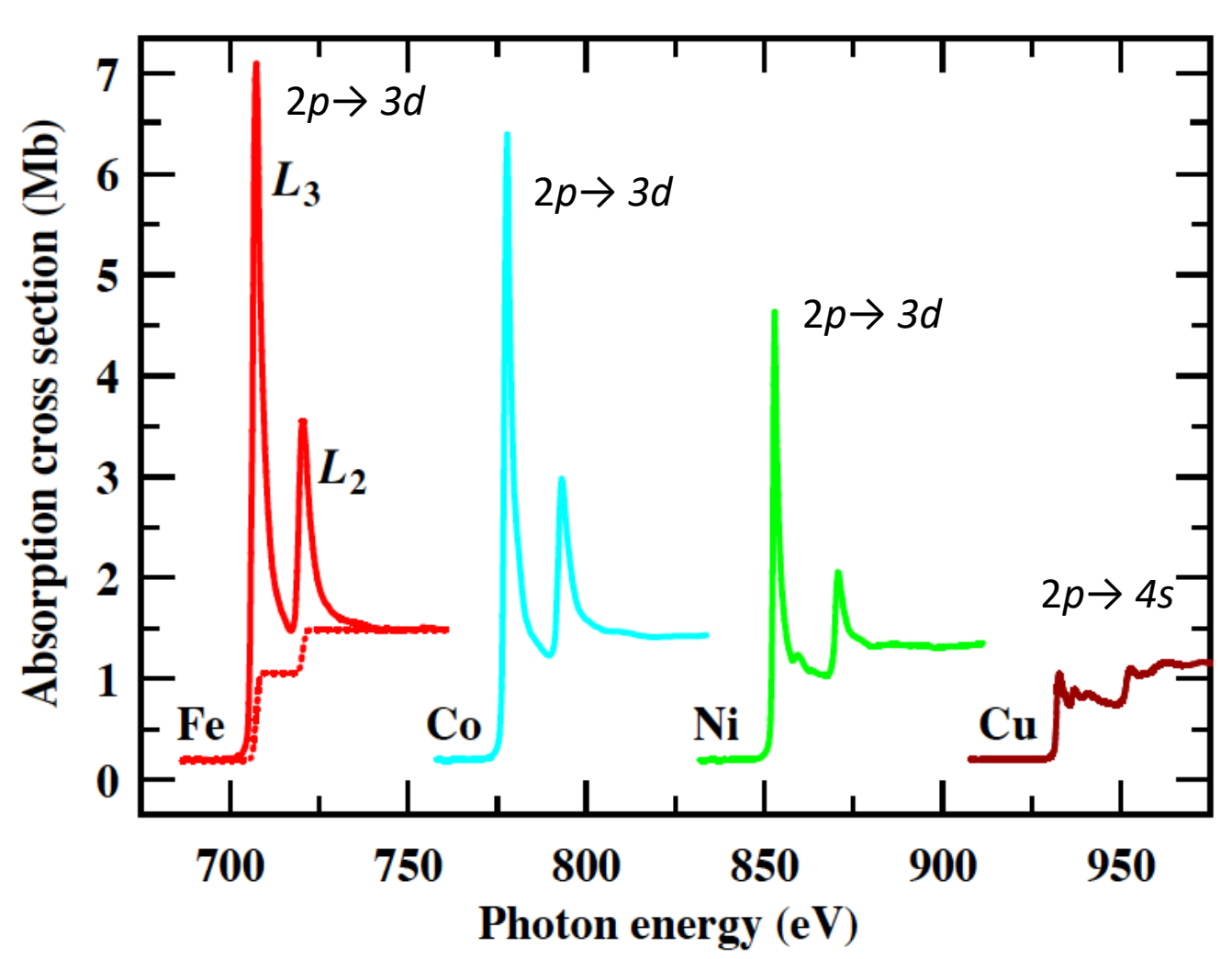
intensity ratio related to degeneracy (2j+1)





#### XAS element sensitivity





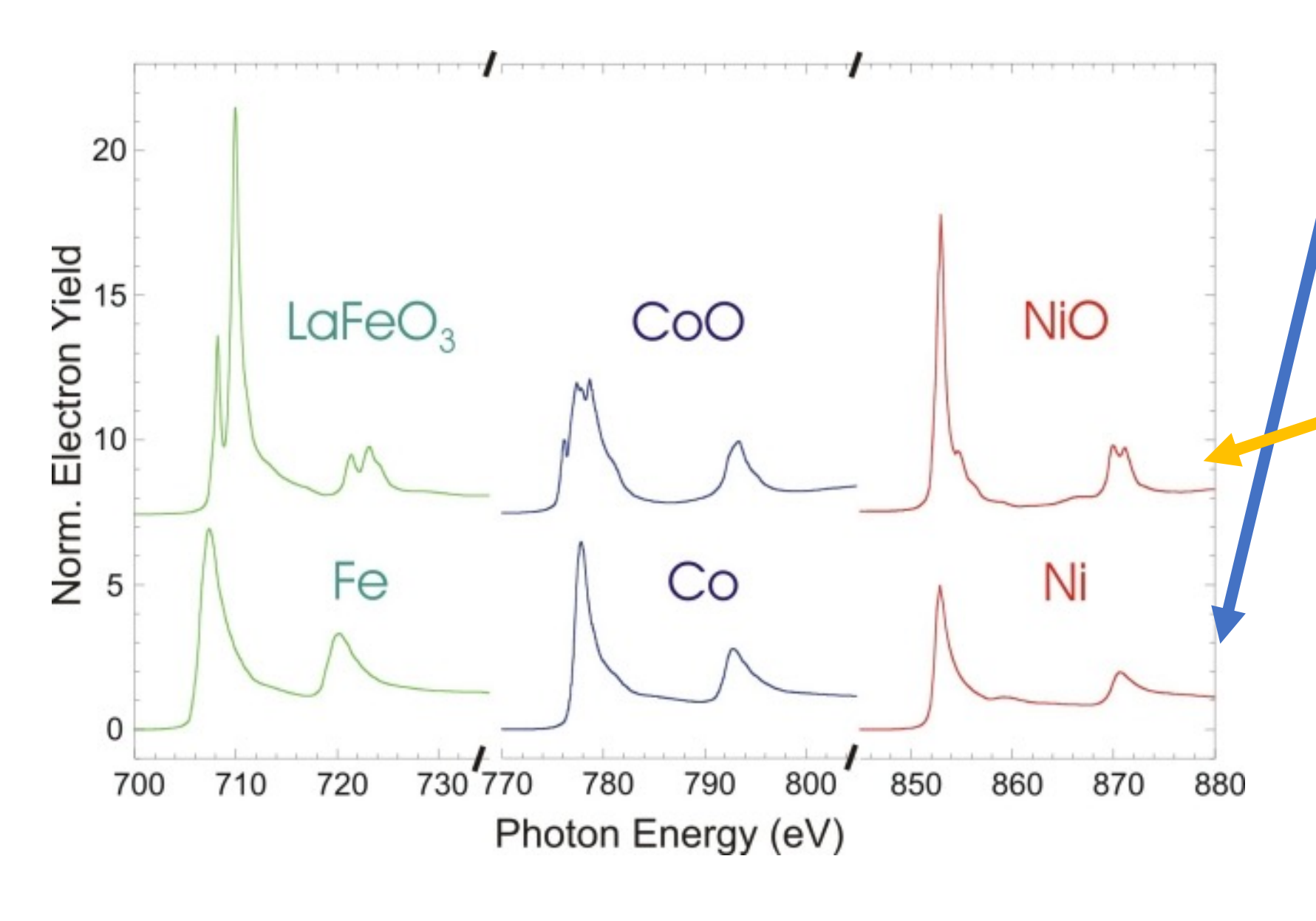
Element	K 1s	L <sub>1</sub> 2s	L <sub>2</sub> 2p <sub>1/2</sub>	L <sub>3</sub> 2p <sub>3/2</sub>
26 Fe	7112	844.6†	719.9†	706.8†
27 Co	7709	925.1†	793.2†	778.1†
28 Ni	8333	1008.6†	870.0†	852.7†
29 Cu	8979	1096.7†	952.3†	932.7

For Fe, Co, Ni, the signal is dominated by the  $2p \rightarrow 3d$  transition

For Cu, the 3d states are fully occupied (except for some weak hybridization), the signal corresponds to  $2p \rightarrow 4s$ 

The observed intensity reflects the empty DOS states between  $E_F$  and  $E_V$ 

#### XAS: chemical shift, crystal field



The metal spectra mainly show two broad peaks, reflecting the width of the empty parts of the d-bands.

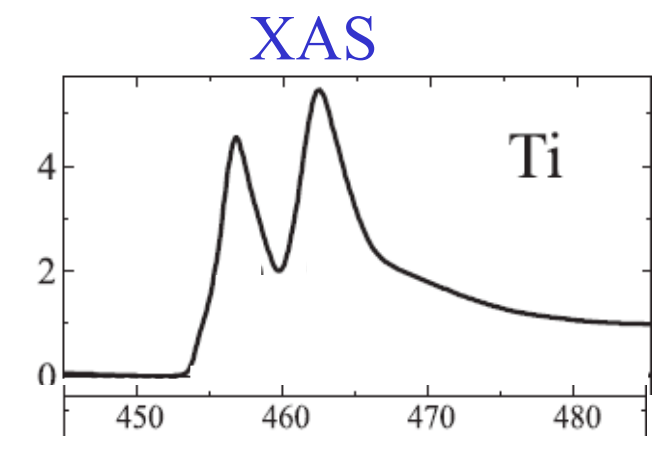
The oxide spectra exhibit fine structure, called multiplet structure. The empty oxide states are more localized than metal states and their energies are determined by crystal field and multiplet effects.

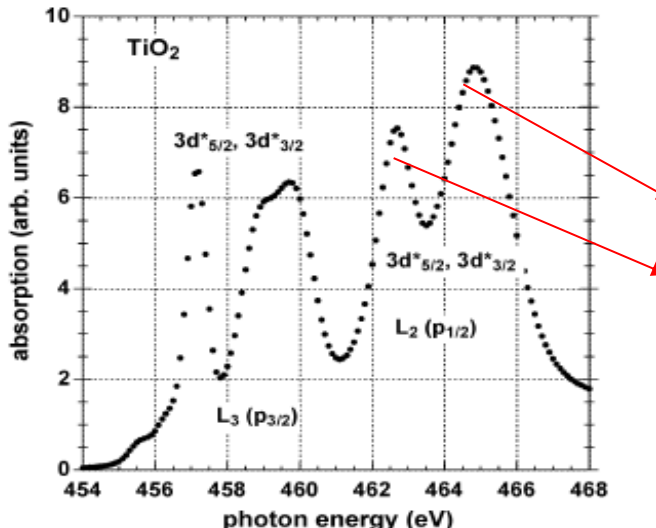
## XAS vs. XPS: example of L<sub>2</sub>, L<sub>3</sub> edges of Ti

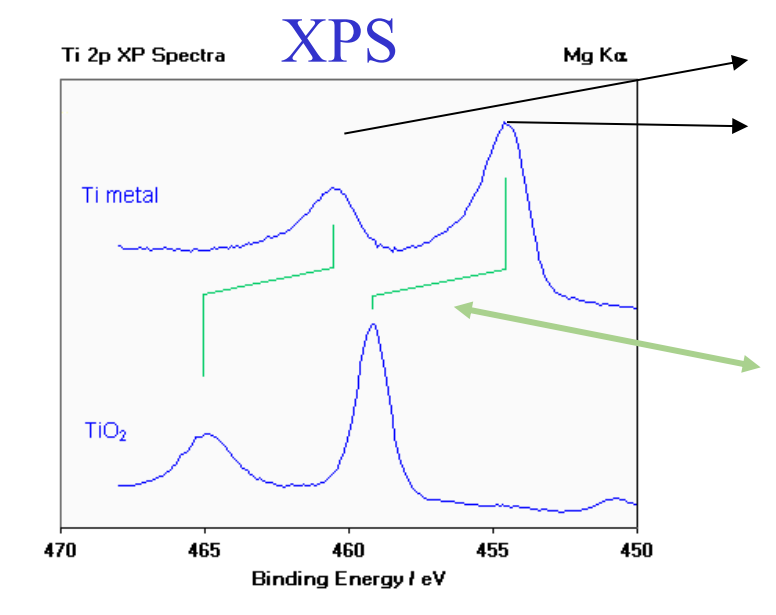
$$\begin{split} H &= H_{atom} + H_{crystal-field} \\ H_{atom} &= \sum \frac{p_i^2}{2m} - \sum \frac{Ze^2}{r_i} + \sum \frac{e^2}{r_{ij}} + \sum \xi(r_i) l_i \bullet s_i \, ; \ \, H_{crystal-field} = -eV(r) \end{split}$$

Chemical shift: crystal field (bonds formation) modifies the electronic cloud around each atom. Both valence and core states are affected

Ti: [Ar] 3d<sup>2</sup> 4s<sup>2</sup>







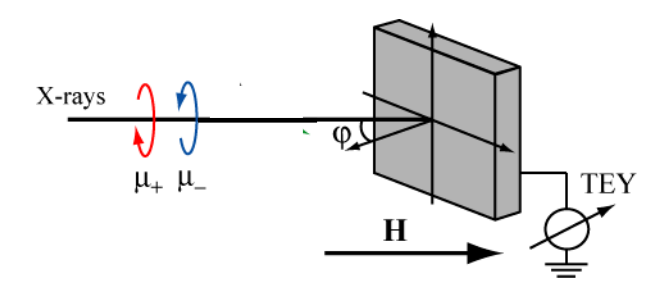
Crystal field and spin-orbit splitting of the 3d valence states:
XAS is sensitive to the valence band

Spin-orbit splitting of the 2p core levels

Chemical shift of core levels: common to both techniques

- The XAS spectrum is a convolution of the core levels and valence states
- 3d valence states are strongly affected by the hybridization with the oxygen atoms (crystal field)

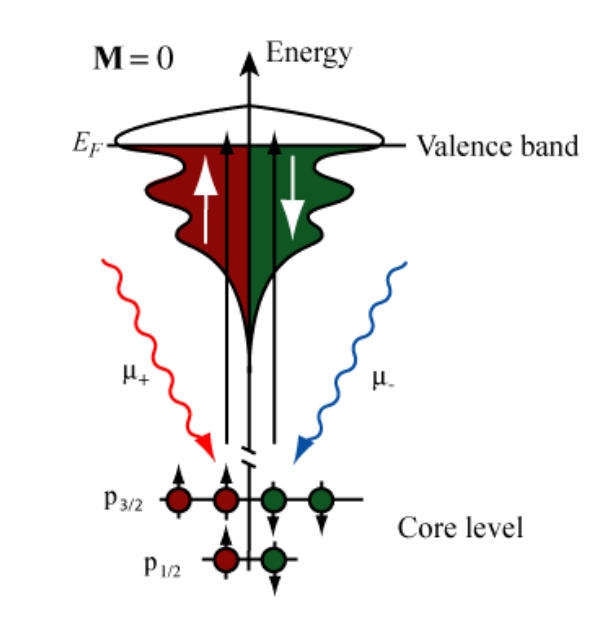
#### XMCD: X-ray magnetic circular dichroism

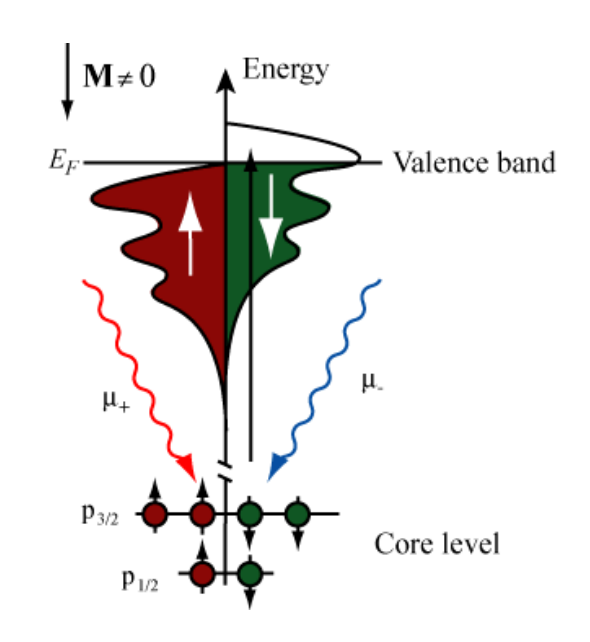


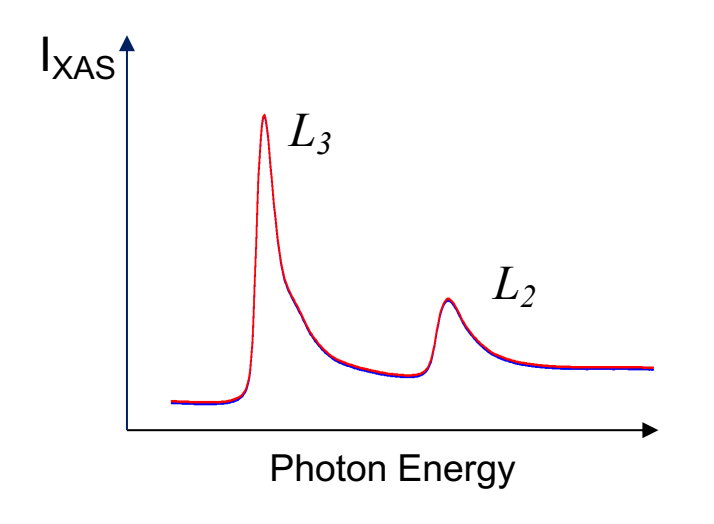
The XMCD, defined as the intensity difference between antiparallel and parallel orientations of the sample magnetization and the incident photon spin, is directly proportional to the atomic magnetic moment.

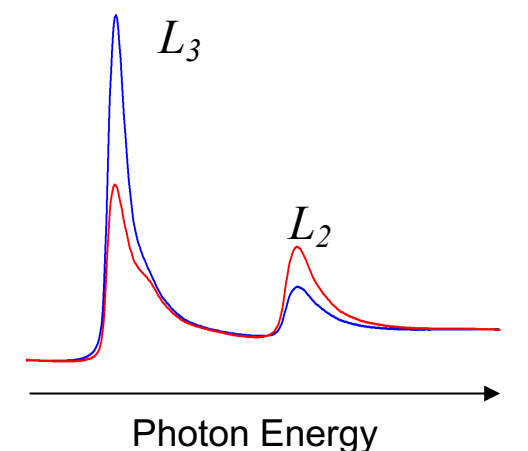
#### Dipole selection rules, for 3d transition metals

$$\Delta l = \pm 1$$
,  $\Delta s = 0$   $2p < \frac{3d}{4s}$   $\Delta m_l = +1$  right circular  $\Delta m_l = -1$  left circular

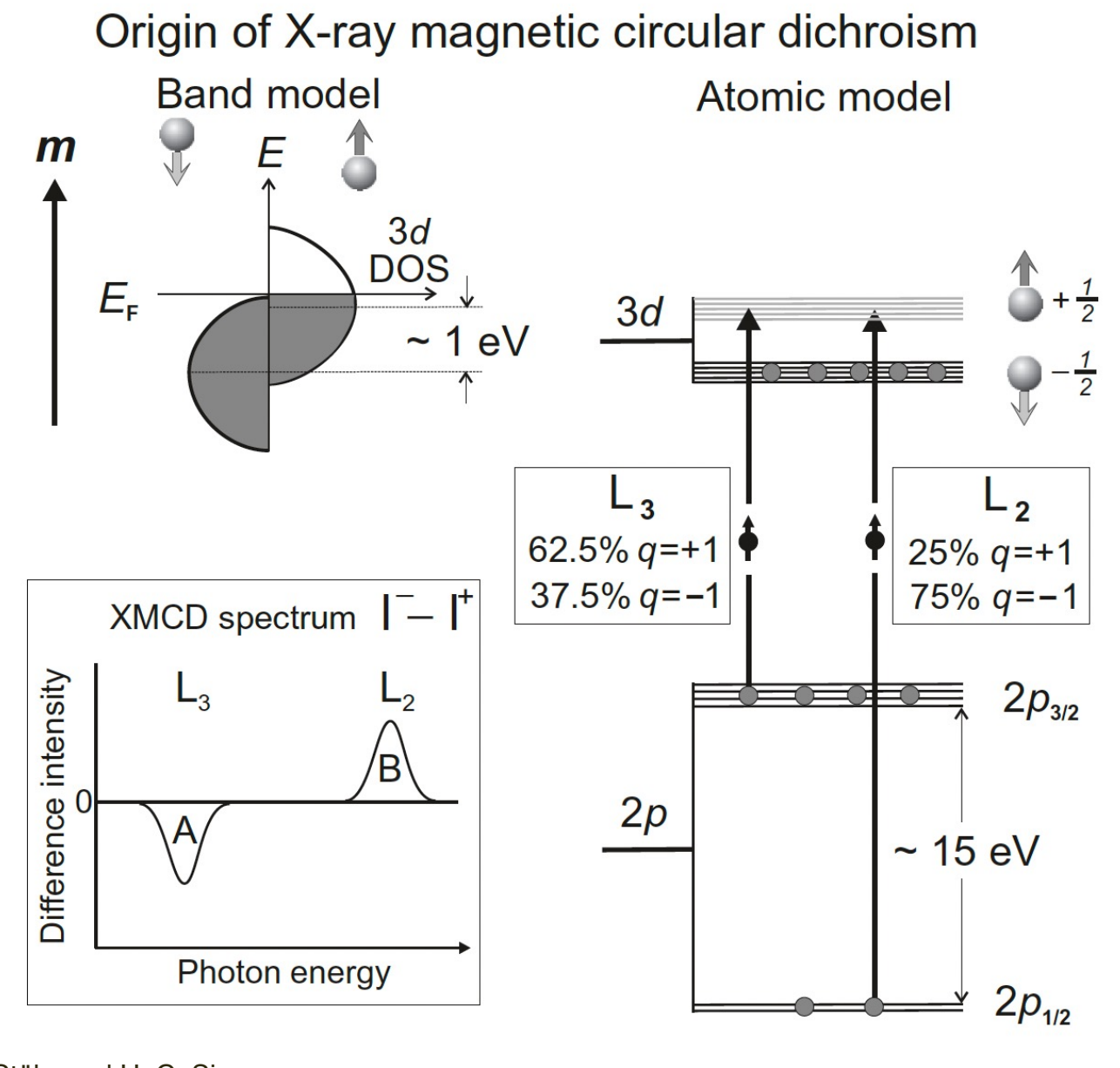








## XMCD: X-ray magnetic circular dichroism



Case of one spin channel fully occupied (strong ferromagnet)

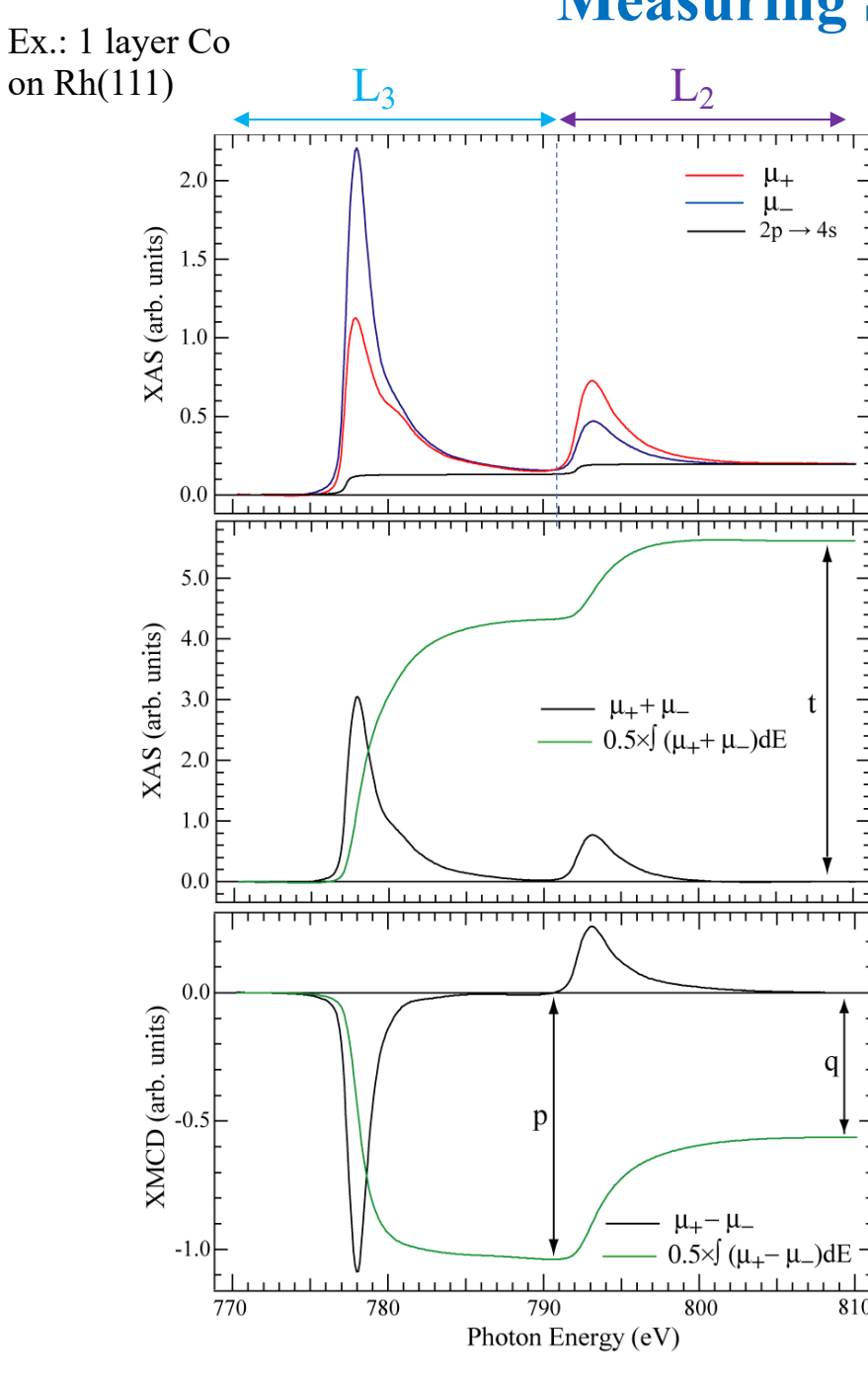
The fraction of up-spin electrons excited from the p core shell through absorption of X-rays with angular momentum  $q = \pm 1$  is listed for the L<sub>3</sub> and L<sub>2</sub> edges

At the L<sub>3</sub> edge, X-rays with positive (q = 1) photon spin excite more spin-up electrons than X-rays with negative (q = -1) photon spin, and at the L<sub>2</sub> edge the opposite is found.

#### Two step model:

- 1) spin-polarized photoelectrons are created by using circularly polarized x-rays
- these polarized photoelectrons are used to analyze the spin-split valence density of states, thus the valence band acts as a spin-sensitive detector.

#### Measuring S and L momenta via XMCD sum rules



#### Sum rules for 3d transition metals:

$$L = -\frac{4}{3}h_d \frac{\int_{L3+L2} (\mu_+ - \mu_-)dE}{\int_{L3+L2} (\mu_+ + \mu_-)dE} = -\frac{4}{3}h_d \frac{q}{t}$$

$$S + 7D = -h_d \frac{6\int_{L3} (\mu_+ - \mu_-) dE - 4\int_{L3+L2} (\mu_+ - \mu_-) dE}{\int_{L3+L2} (\mu_+ + \mu_-) dE}$$
$$= -h_d \frac{6p - 4q}{t}$$

Here the notation is 
$$I\mu_+ \rightarrow \mu_+$$
  $I\mu_- \rightarrow \mu_-$ 

L: orbital angular momentum

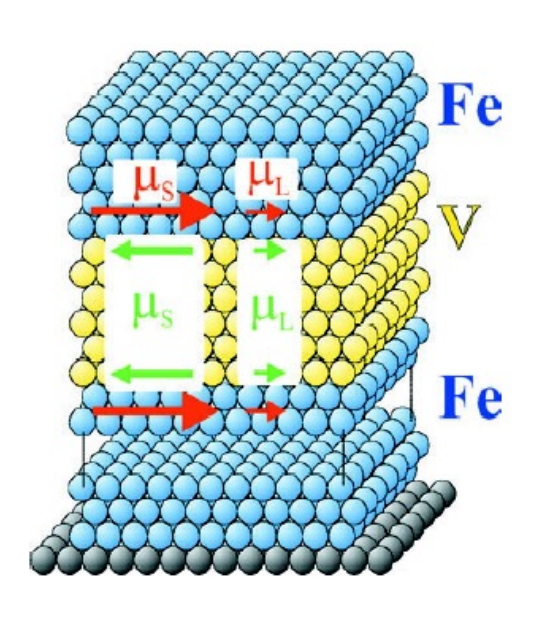
S: spin angular momentum

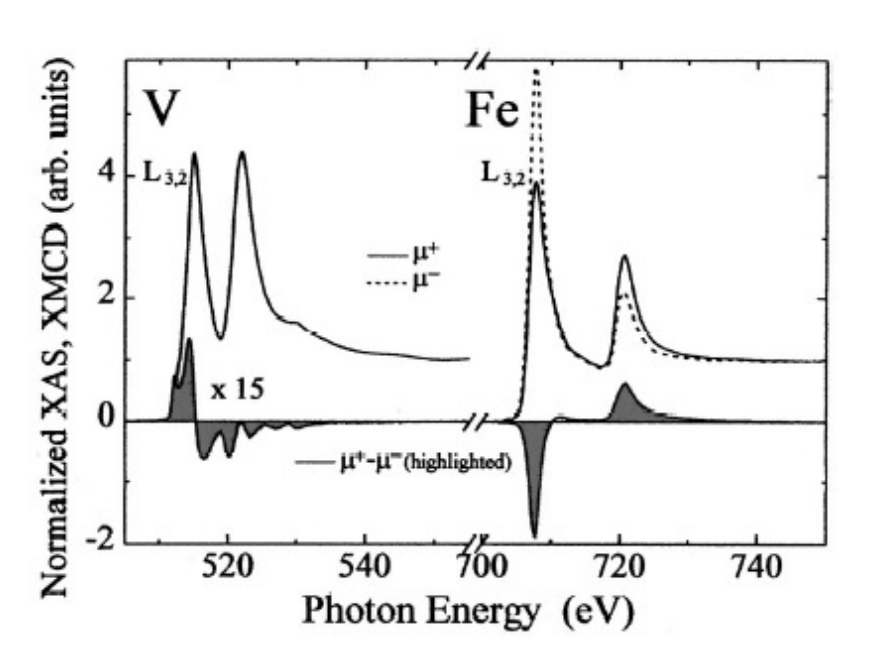
*D*: magnetic spin dipole

 $h_d$ : number of d-holes (empty states) in the valence band (frequently unknown, requires input from theory) L, S in units of  $\mu_B$  / atom

$$r = \frac{L}{S + 7D}$$
 This value is independent on  $h_d$  and can be easily compared for different samples

#### **Element resolved magnetism**

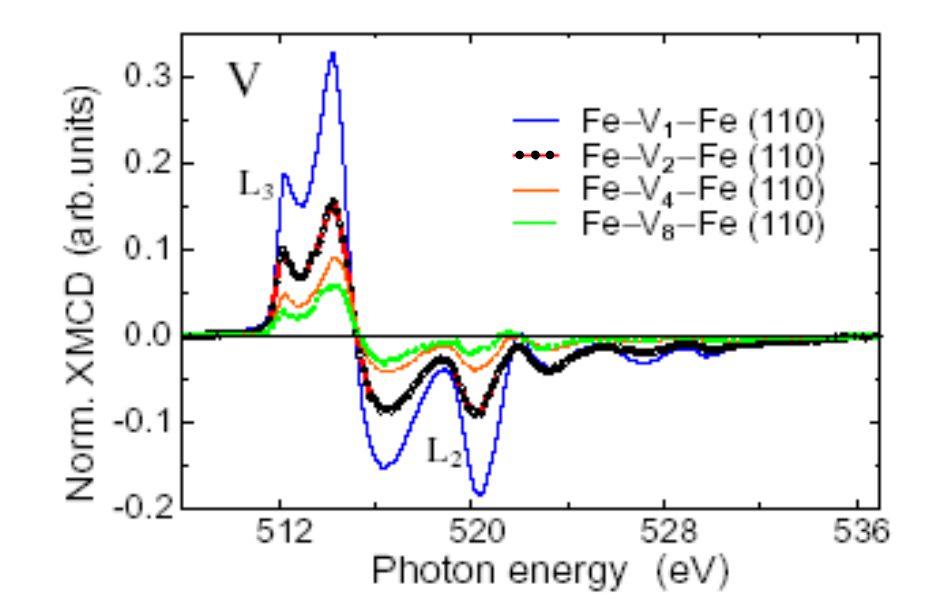




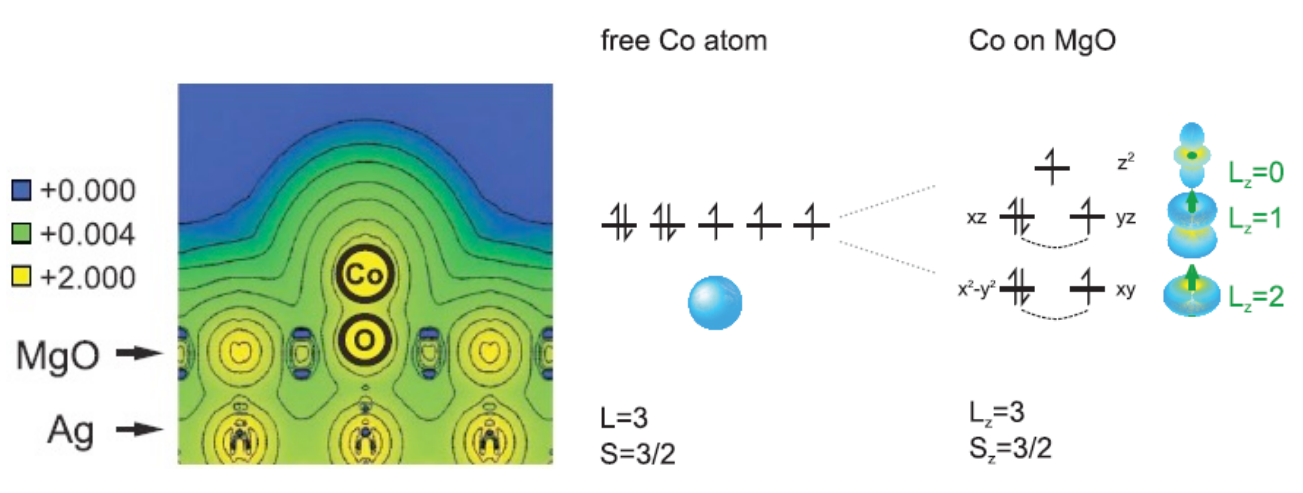
Normalized XAS of left (dashed line) and right (solid line) circularly polarized light and the XMCD at the  $L_{2,3}$  edges of V and Fe for a Fe/V4 /Fe(110) trilayer structure.

- 1) Stronger magnetic moments in Fe compared to V
- 2) Antiferromagnetic coupling: XMCD signal for V and Fe have opposite signs

The induced magnetic moment in the V atoms strongly reduces with increasing the V thickness



#### Reaching the MAE limit in 3d metal atoms

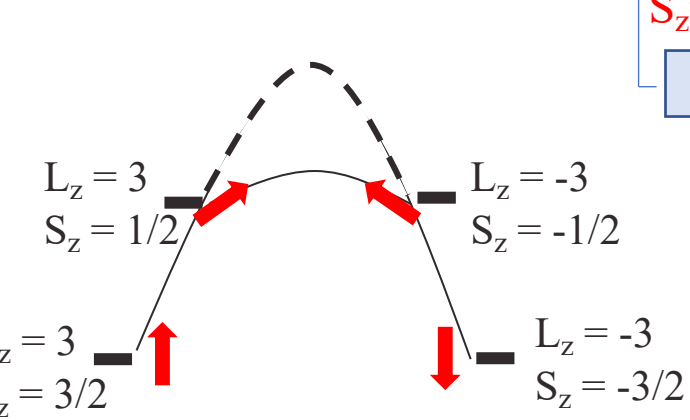


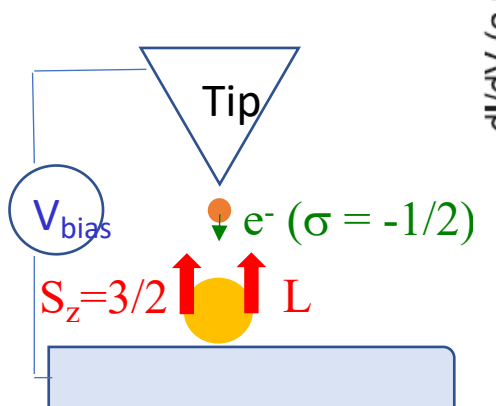
Co atom on MgO adsorbs on top of oxygen and forms a strong uniaxial bond preserving atomic values of L and S

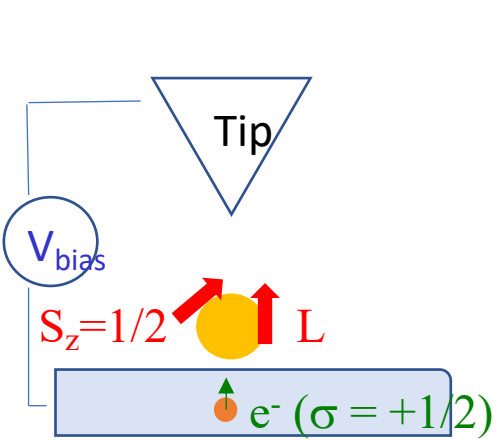
#### From XMCD:

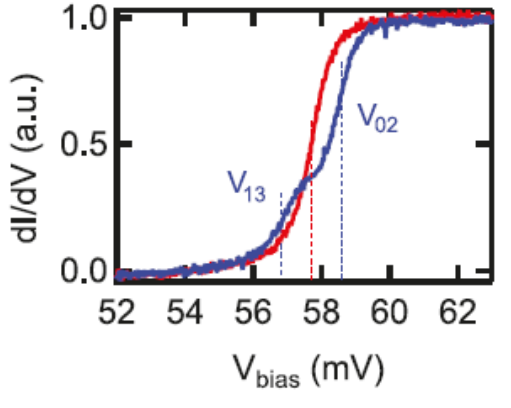
- $L_z = 2.9$ ;  $S_z = 3/2$
- The uniaxial bond generates a strong out-of-plane anisotropy

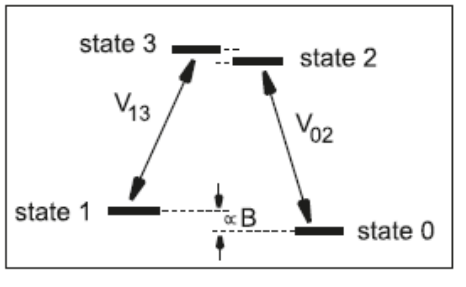
- To reverse we need  $\Delta S_z = 1$ .
- Different from the classical case where the magnetization goes through the  $S_z=0$  state ( $\Delta S_z=3/2$ )









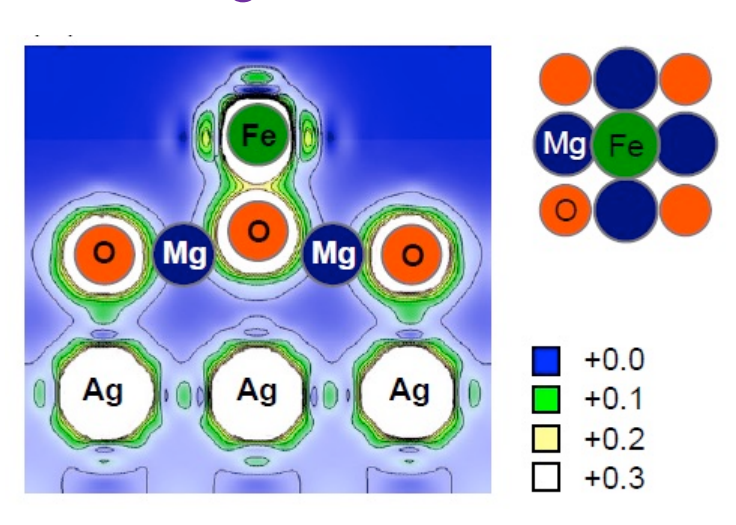


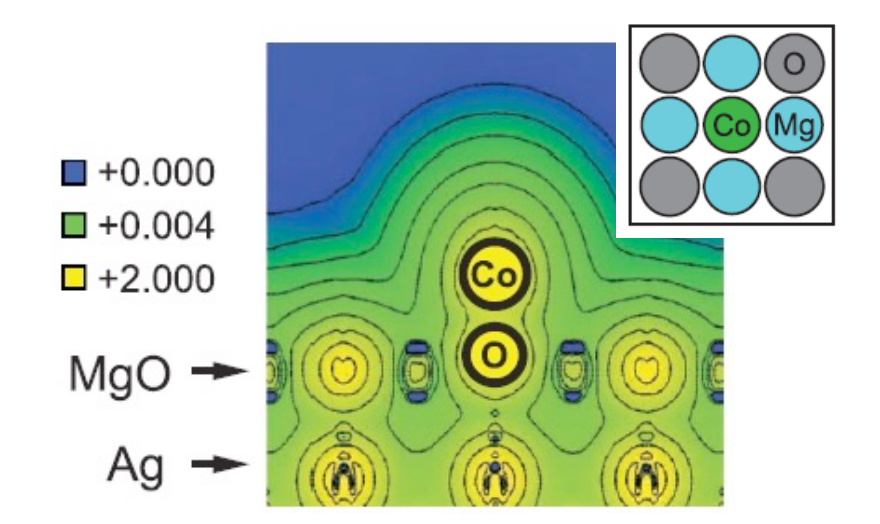
$$eV_{bias} = \lambda \Delta S_z L$$
  
 $\lambda \sim 22 \text{ meV}$   
SO coupling param.

$$\Delta \sigma = 1 \rightarrow \Delta S_z = -1$$

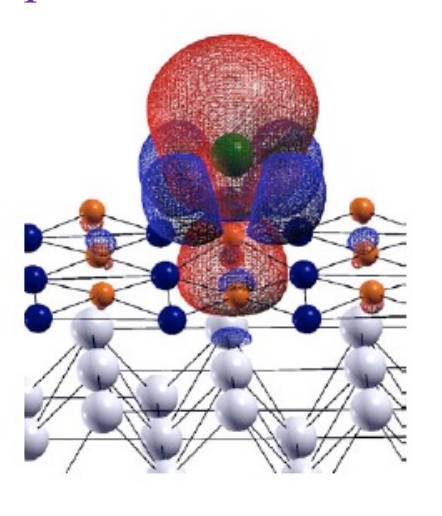
## Fe, Co atoms adsorbed on MgO/Ag(100)

#### Charge distribution



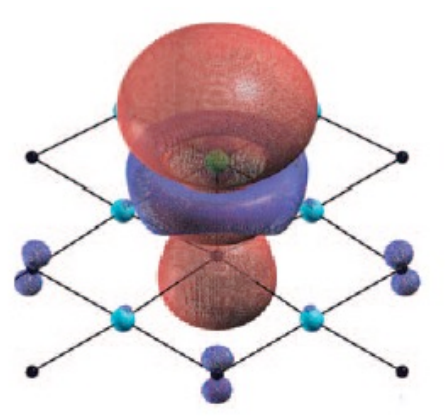


#### Spin distribution from DFT



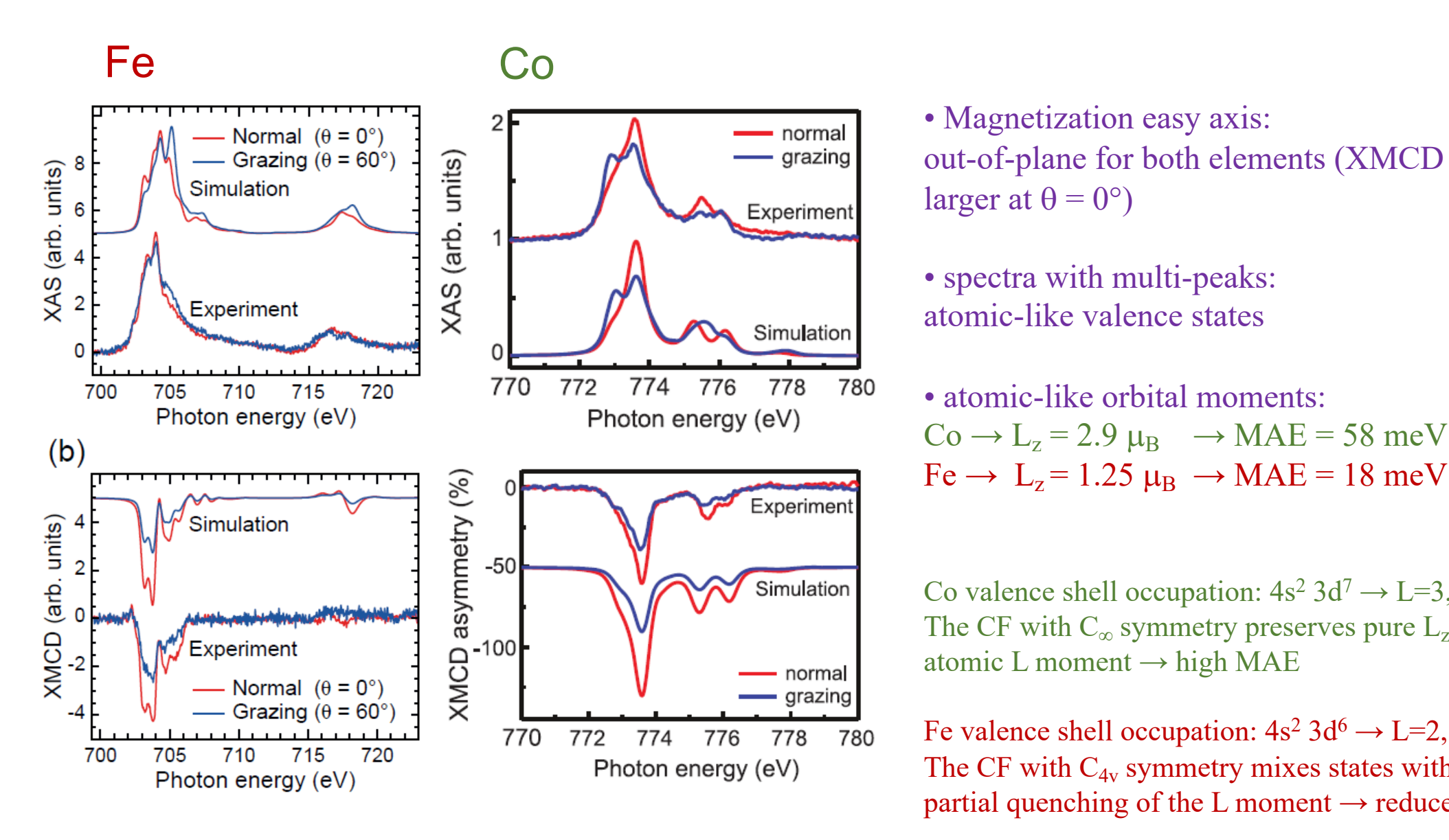
C<sub>4v</sub> crystal field (ellipsoidal with 4 ears spin distribution)

Majority Minority



Axial  $(C_{\infty})$  crystal field (ellipsoidal spin distribution)

#### XMCD of Fe, Co atoms adsorbed on MgO/Ag(100)



- Magnetization easy axis: out-of-plane for both elements (XMCD signal larger at  $\theta = 0^{\circ}$ )
- spectra with multi-peaks: atomic-like valence states
- atomic-like orbital moments:  $Co \rightarrow L_z = 2.9 \ \mu_B \rightarrow MAE = 58 \ meV$

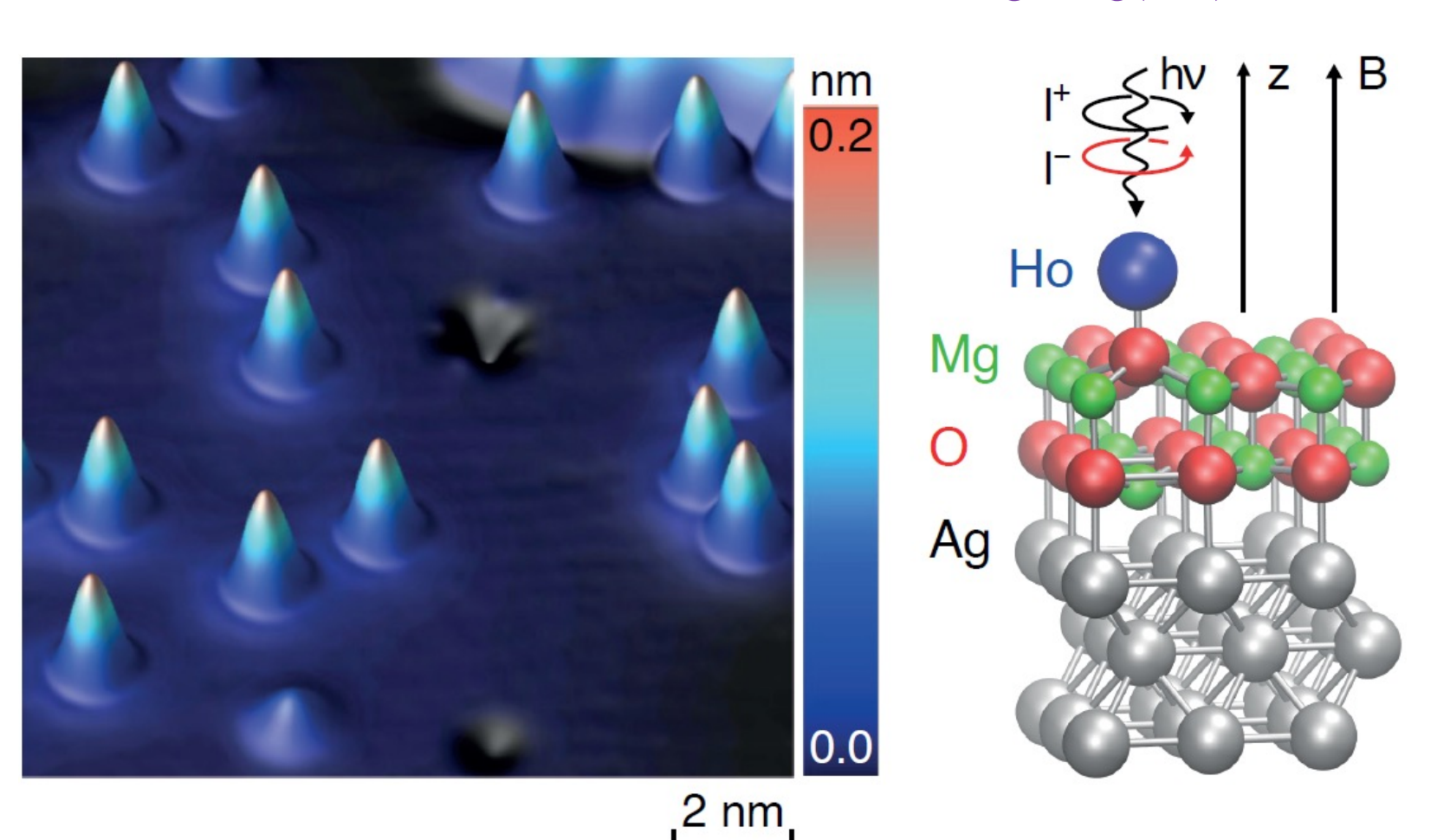
Co valence shell occupation:  $4s^2 3d^7 \rightarrow L=3$ , S=3/2. The CF with  $C_{\infty}$  symmetry preserves pure  $L_7$  states  $\rightarrow$ atomic L moment  $\rightarrow$  high MAE

Fe valence shell occupation:  $4s^2 3d^6 \rightarrow L=2$ , S=2. The CF with  $C_{4v}$  symmetry mixes states with  $\Delta L_z = 4 \rightarrow$ partial quenching of the L moment → reduced MAE

$$B = 7 T$$
 and  $T = 2 K$ 

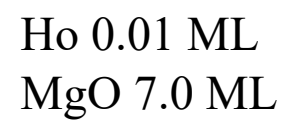
## Single atom magnets

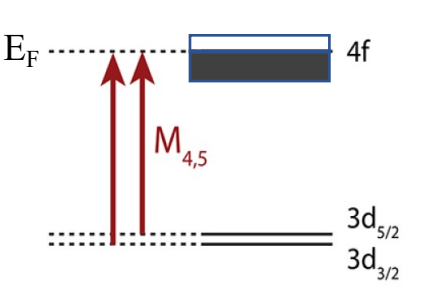
#### Holmium atoms on MgO/Ag(100)



Ho adsorbs on top of Oxygen: CF almost axial with small  $C_{4v}$  contribution

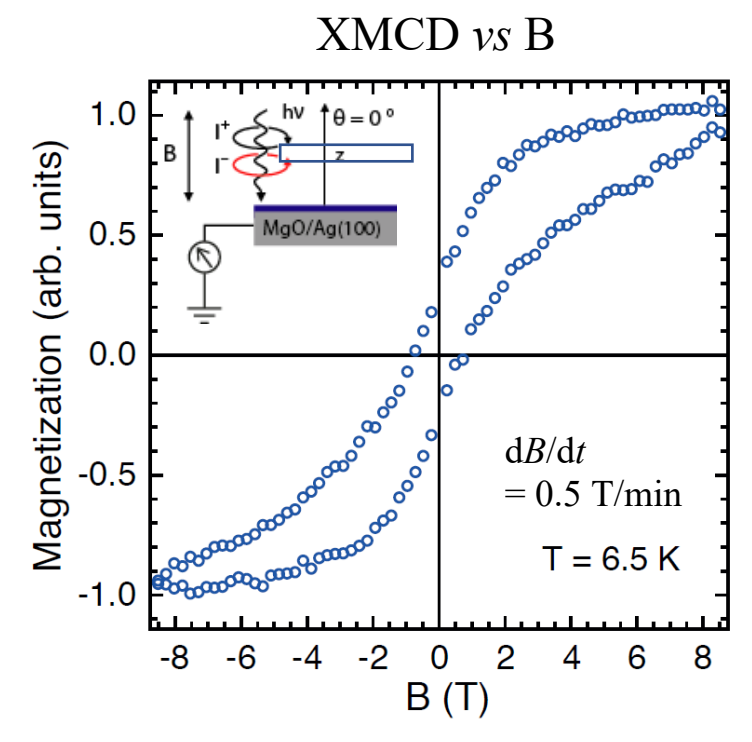
Ho: 
$$4f^{10}$$
  
 $S=2, L=6$   
 $J=8$ 



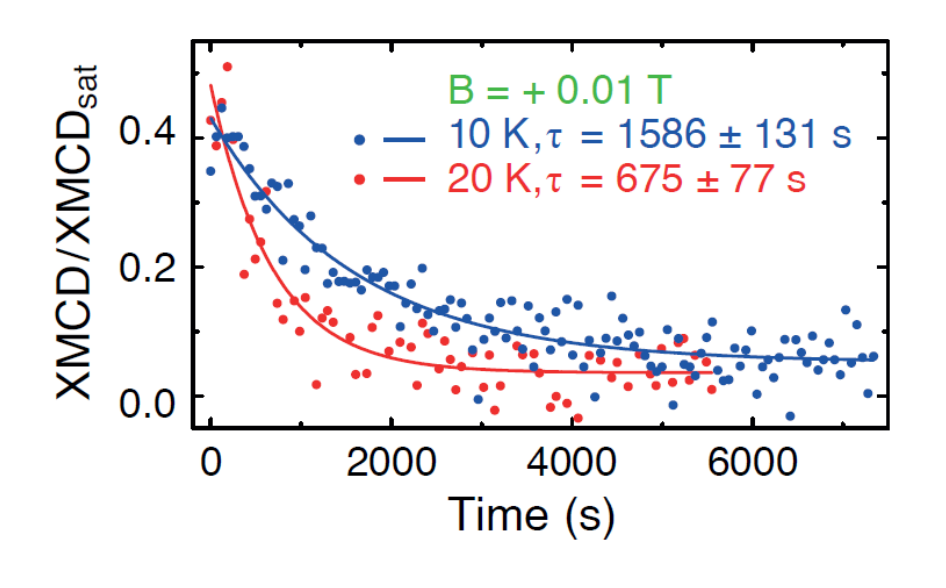


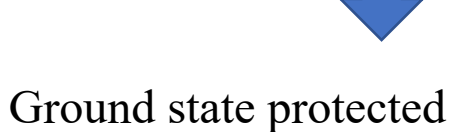
## Single atom magnets

 $M_{4,5}$  edge (3d  $\rightarrow$  4f) XAS (arb. units) XMCD (arb. units) B = 8.5 TT = 6.5 K1340 1350 1360 1370 1380 1390 Energy (eV)



XMCD vs t (after saturation at 6.8 T)





MgO is insulating

MgO is very stiff

-> No QTM in C<sub>4v</sub> crystal field

-> no spin-electron scattering

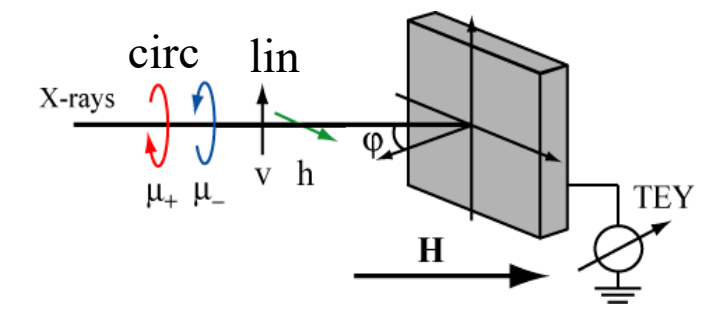
-> reduced spin-phonon scattering



- Magnetic hysteresis up to 9 T
- 30% remanence at B=0 T
- coercive field of about 1 T
- long spin life time up to 40 K

#### XLD: x-ray linear dichroism

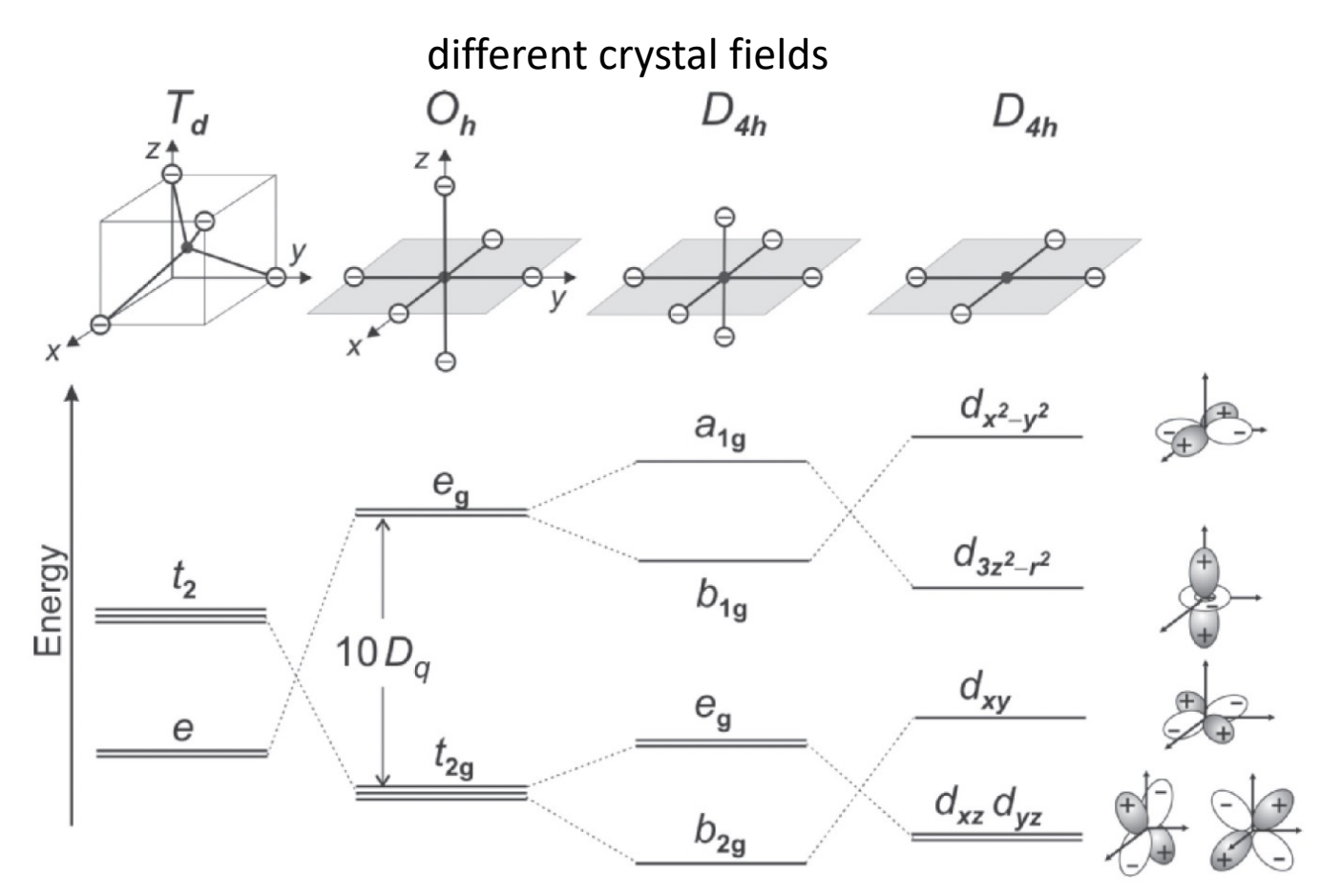
XMLD (magnetic XLD)



# XNLD: natural XLD Linear dichroism is sensitive to charge anisotropy → bond orientation

The dependence of the X-ray absorption intensity on E-vector orientation is then entirely determined by the spatial distribution of the empty valence states.

The X-ray absorption intensity is maximum when E is aligned along the orbital and is zero when E lies in the nodal plane.



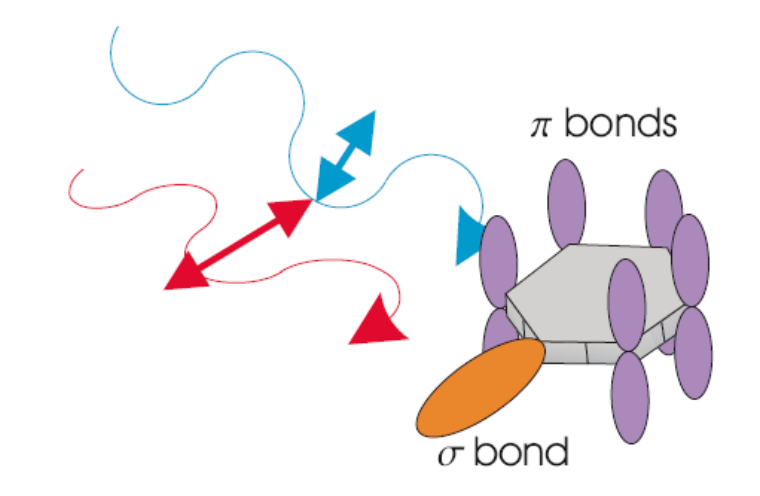
#### **XLD:** x-ray linear dichroism

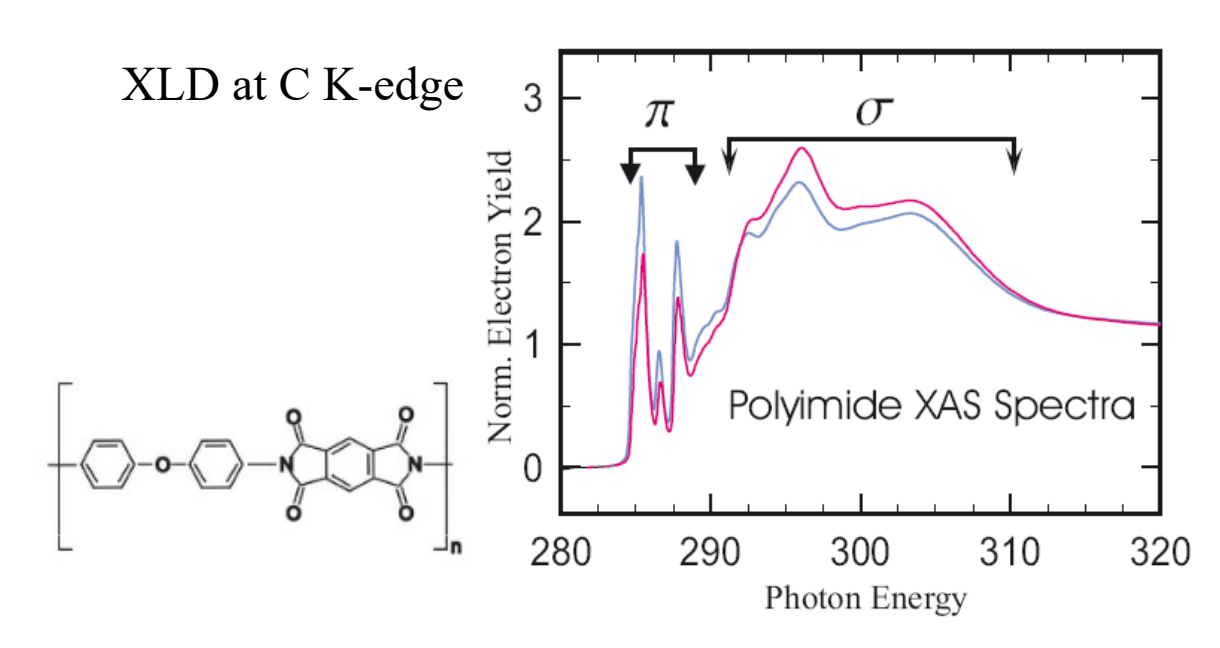
XNLD: natural XLD

Linear dichroism is sensitive to charge anisotropy

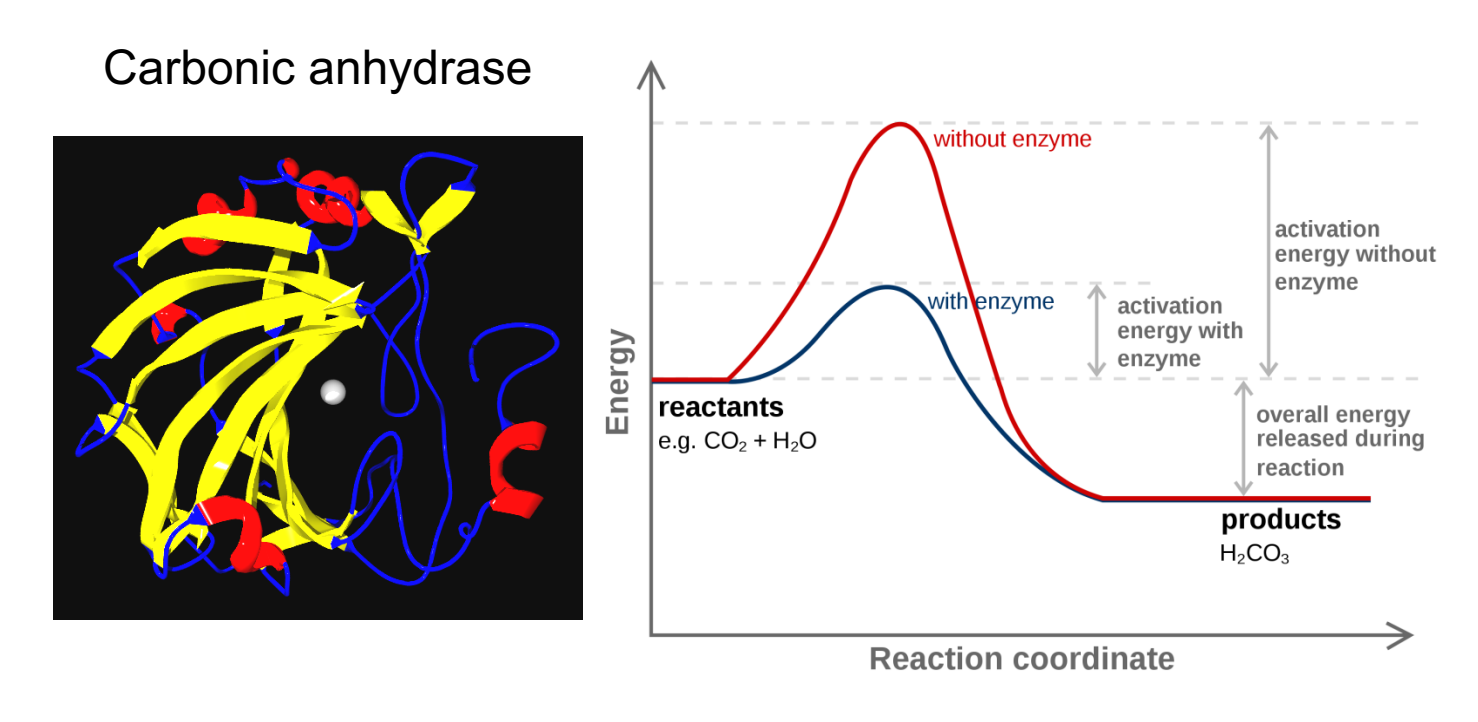
→ bond orientation

#### application to molecular systems





## Enzymes are proteins that catalyse (i.e., increase the rate of) chemical reaction



Interconvert carbon dioxide and carbonic acid to maintain acid-base balance in blood and other tissues, and to help transport carbon dioxide out of tissues.

$$CO_2 + H_2O \xrightarrow{Carbonic \ anhydrase} H_2CO_3$$
 (in tissues with high  $CO_2$  concentration)

$$H_2CO_3 \xrightarrow{Carbonic anhydrase} CO_2 + H_2O$$

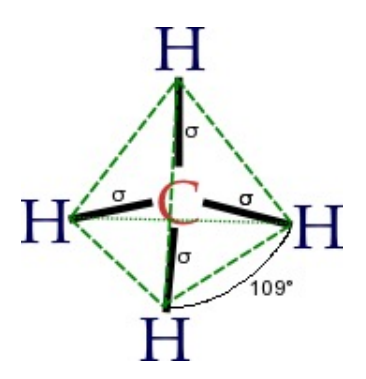
(in lungs with low CO<sub>2</sub> concentration)

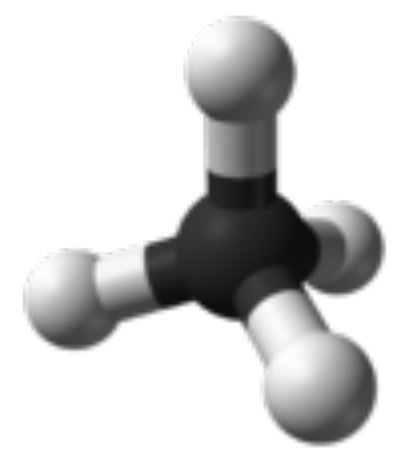
In humans the process works nicely Can we understand how it works?

Increasing the rate of chemical reaction is important for industrial applications

#### Oxidation of methane to methanol

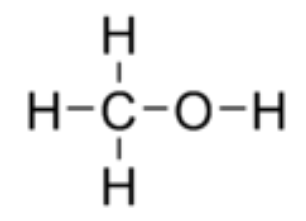
#### methane

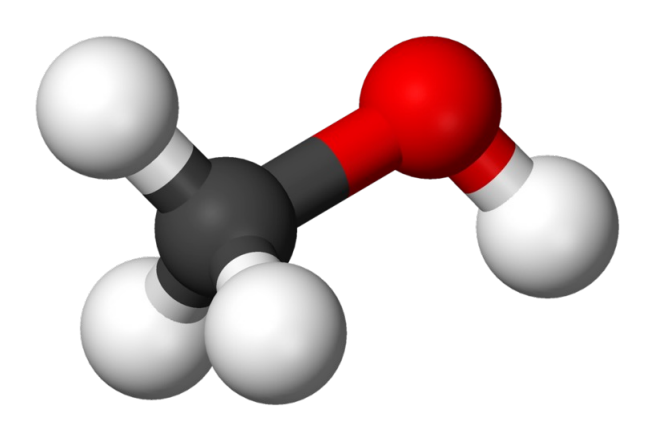




Gas
Explosive
Huge amount
Greenhouse gas

#### methanol





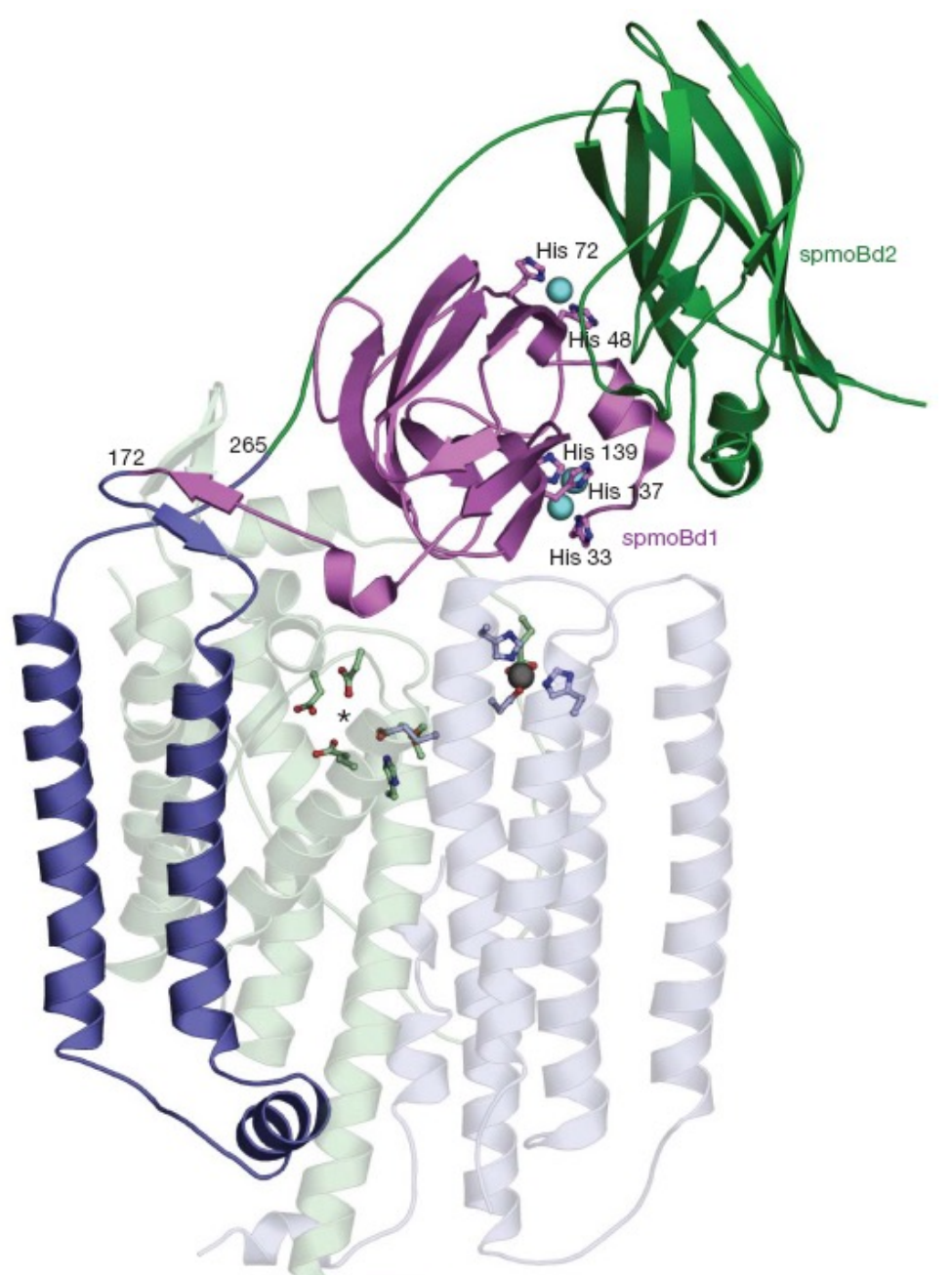
Liquid Easy to storage Fuel

The methane oxidation is a difficult and expensive reaction because the methane is the most inert hydrocarbon

#### however

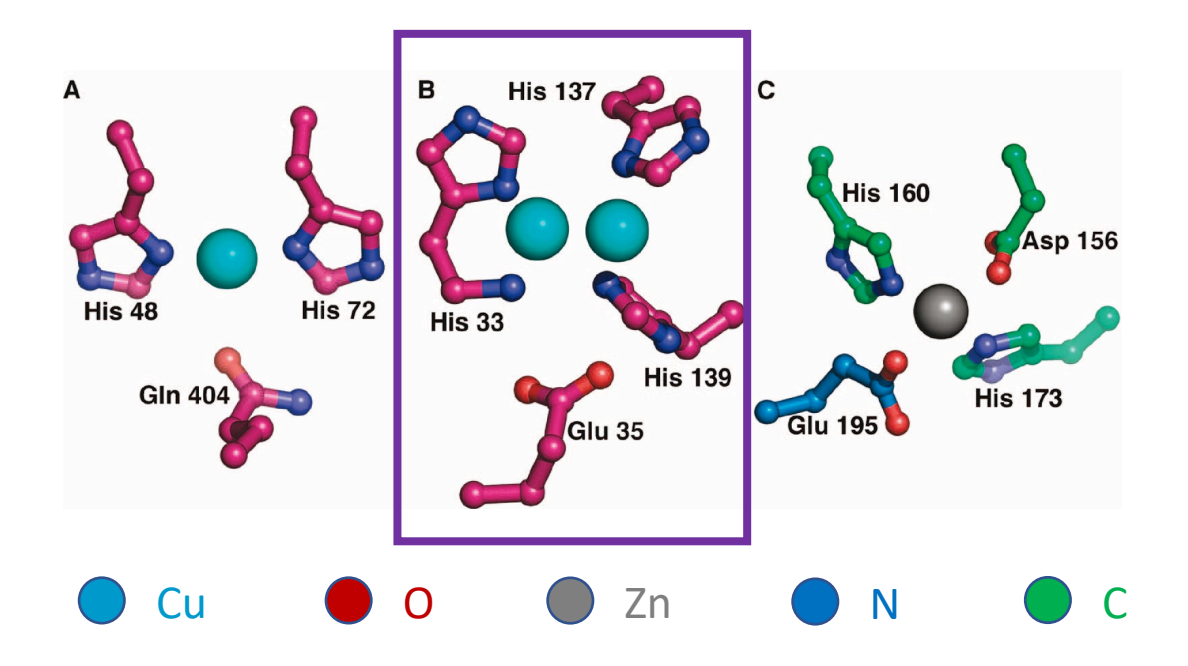
Methanotrophs bacteria use methane monooxygenase (MMO) enzymes to convert methane to methanol at ambient conditions !!!

## monooxygenase (MMO)



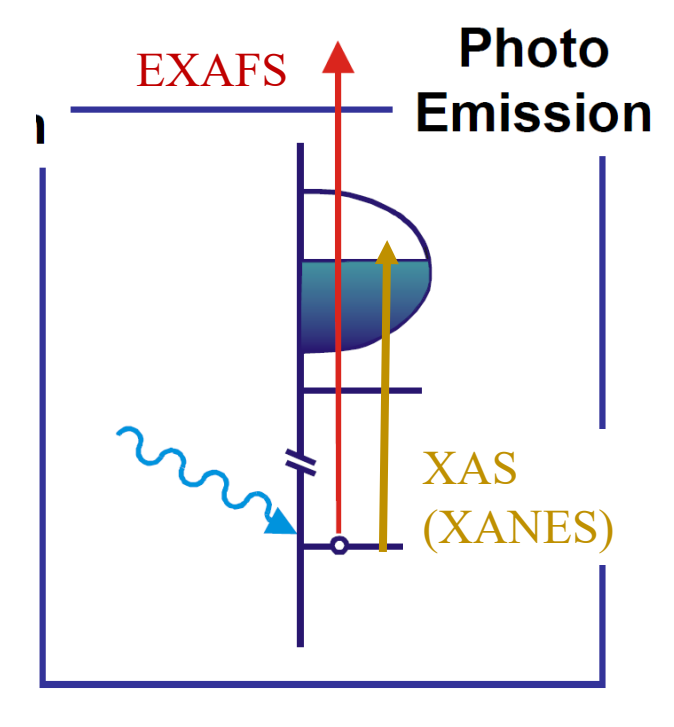
MMO metal centers.

- (A) Mononuclear copper center.
- (B) Dinuclear copper center.
- (C) Zinc center.



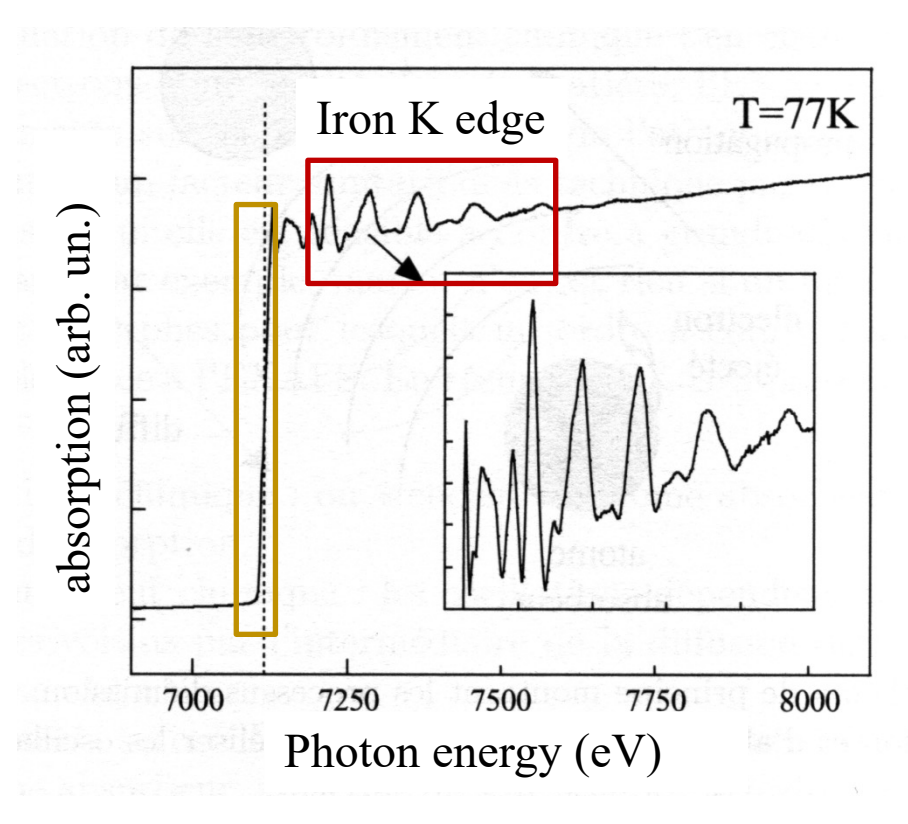
Studying the relative positions of the atoms in these metallic centers, EXAFS reveals that oxidation happens at metal center B

# **EXAFS: Extended X-rays absorption fine structure**



Incoming photons of variably tuned energy

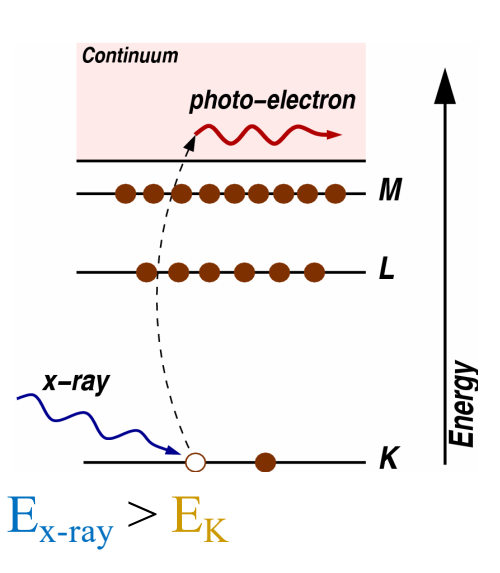
$$E_{x-ray} > E_{edge}$$

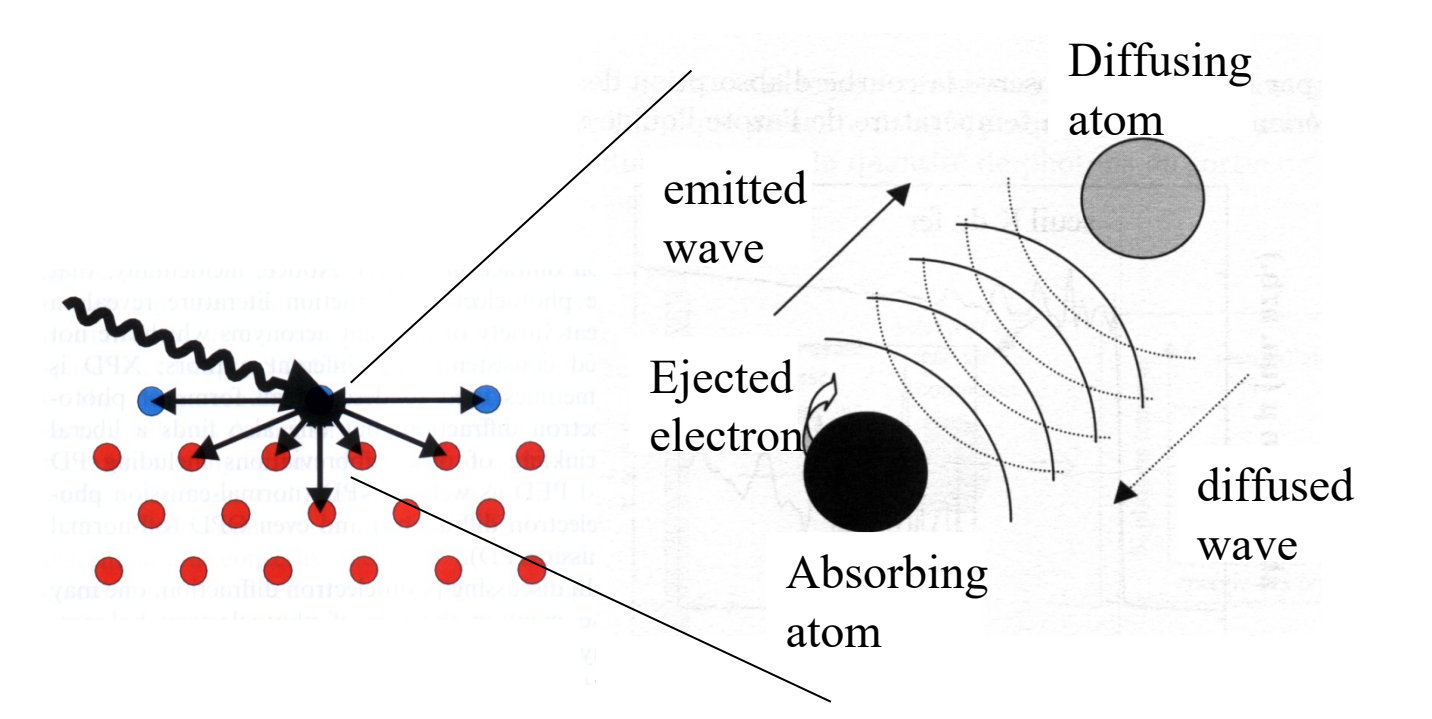


## EXAFS: working principle

## Principle:

- 1) photon in electron out
- 2) The electron (described as a wave) is diffused by neighboring atoms
- 3) Interference between emitted and diffused wave
- 4) The absorption depends on the interference

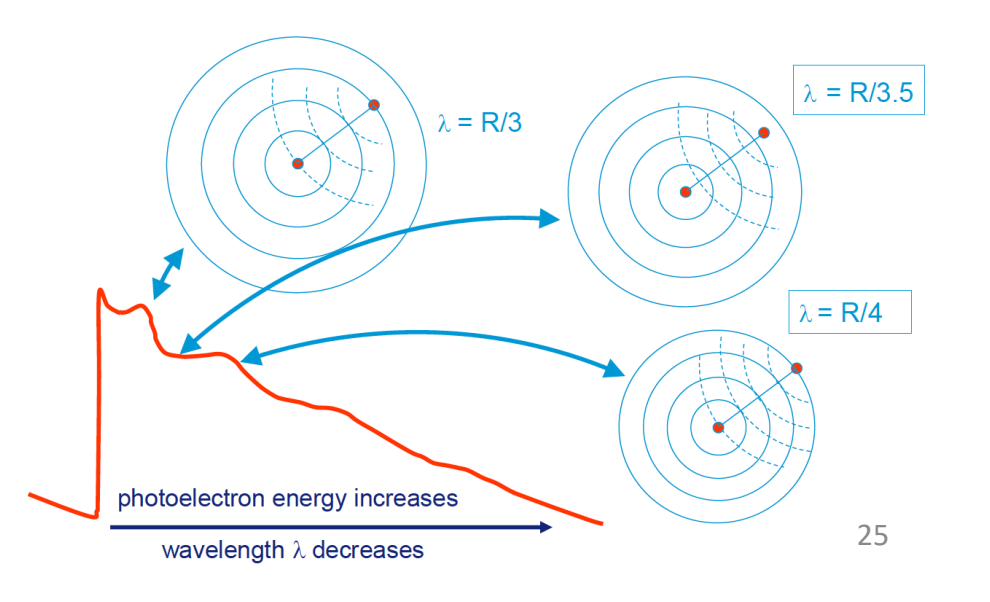


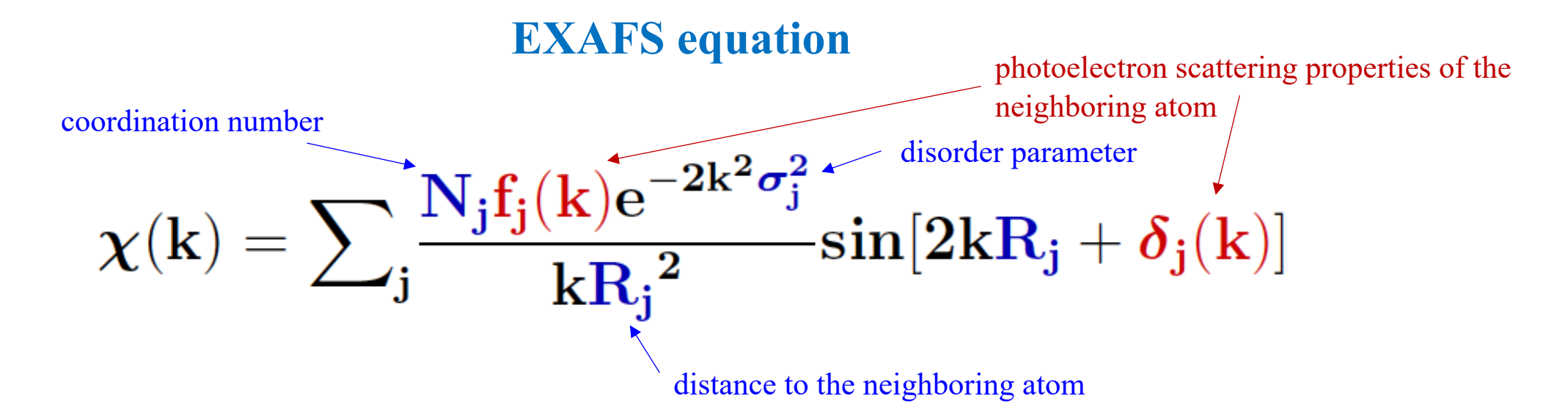


Interference between emitted and diffused wave is constructive or destructive depending on:

- 1) The distance between the absorbing and diffusing atoms → information on the crystallographic structure
- 2) The reflection coefficient of the diffusing atom → information on the chemical environment
- 3) The wavelength  $\lambda$  of the emitted electron  $\rightarrow$  depends on the incoming photon energy

$$E_{kin} = h\nu - E_{edge} = \hbar^2 k^2 / 2m = h^2 / (2m\lambda^2)$$





EXAFS gives information about the local environment (up to ca. 6 Å) around a specific type of absorber atom

- distance to neighboring atoms
- type of neighboring atoms
- number of neighboring atoms

EXAFS is independent of long range order

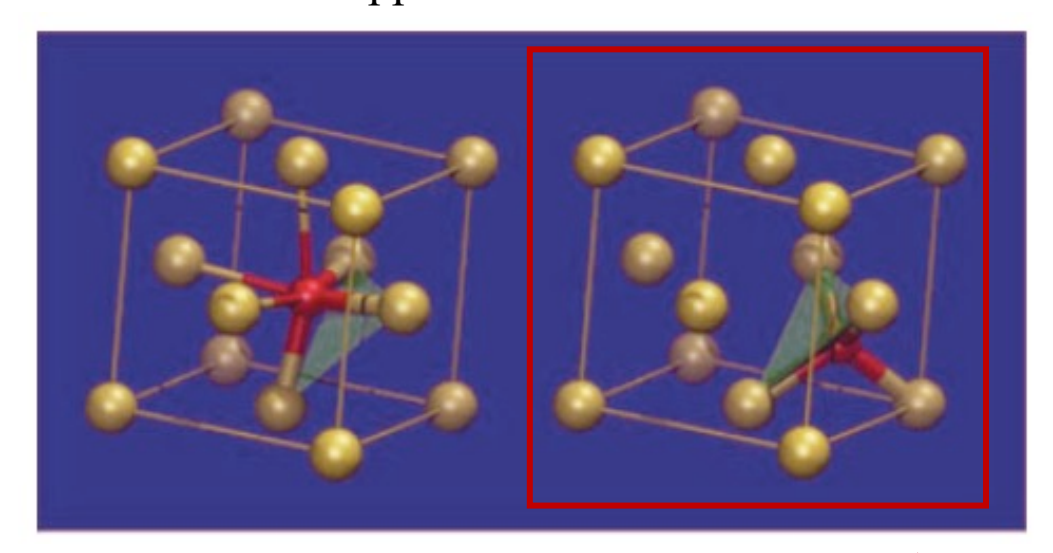
- complementary to diffraction
- works on gases, liquids, amorphous and crystalline solids
- works on highly dispersed phases

EXAFS data analysis requires several steps including FFT to go from reciprocal space (k-space) to real space

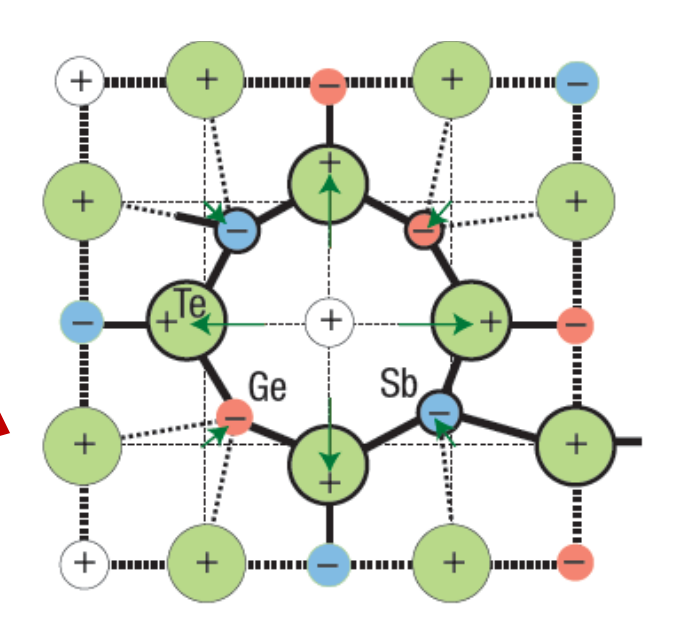
# Understanding the phase-change mechanism of rewritable optical media

Chalcogenide glasses, ex.  $Ge_2Sb_2Te_5$  (GST) can be repeatedly switched between crystalline (c) and amorphous (a) states by application of electrical pulses.

Different reflectivity depending on the crystal structure:  $amorphous \rightarrow matt$  and  $crystalline \rightarrow transparent$  Possible device applications.



Local structure of GST around Ge atoms in the crystalline (left) and amorphous (right) states. Stronger covalent bonds are shown as thicker lines whereas weak interblock bonds are shown as thinner lines.



The crystal structure of laseramorphized GST. A schematic two dimensional image of the lattice distortion of the rocksalt structure due to charge redistribution between the constituent elements; atoms that form the building block of the GST structure are shown using thick lines. The arrows indicate displacements of atoms from the ideal rocksalt positions.

#### **EXAFS** on **GST**

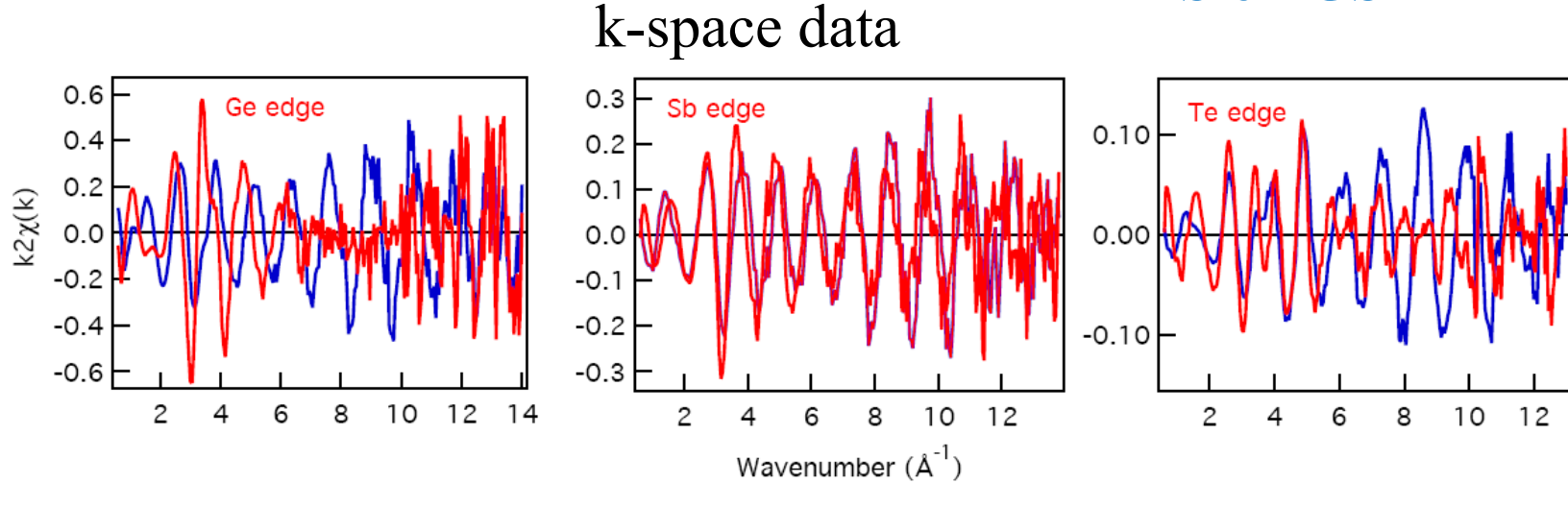
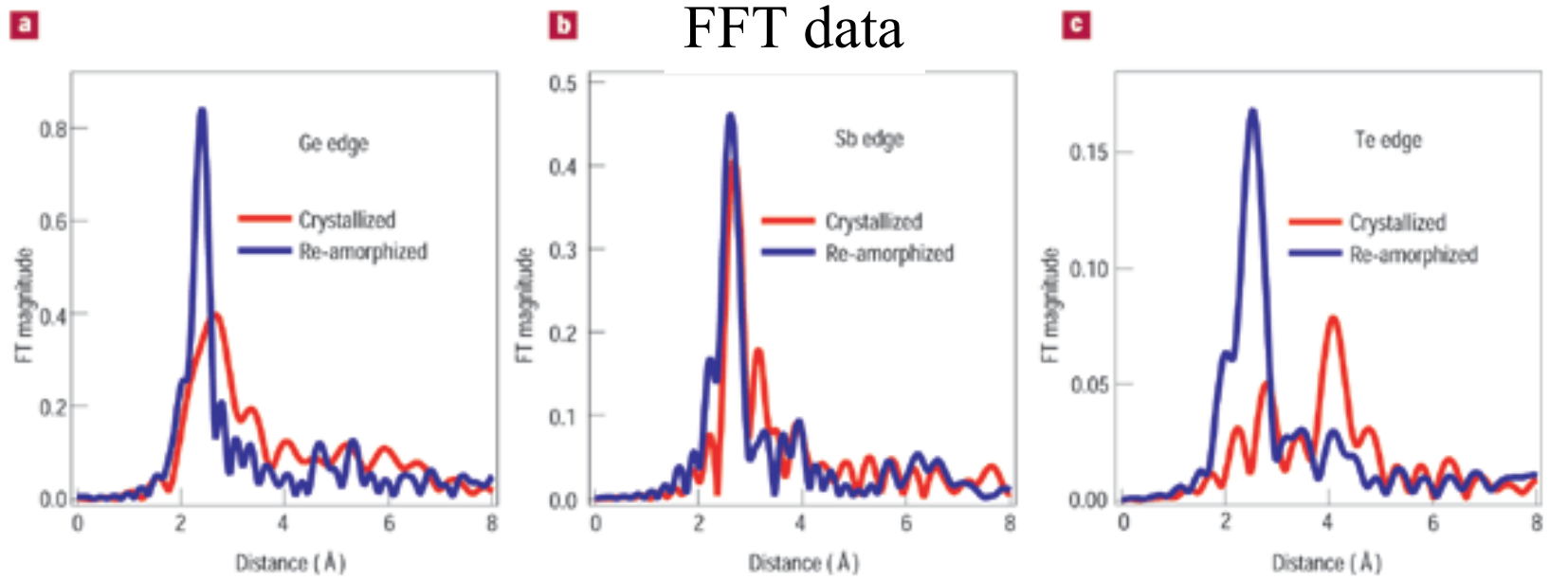


Table 1 Comparison of the GST bond lengths determined from EXAFS and XRD analysis for the crystalline and laser-amorphized states.

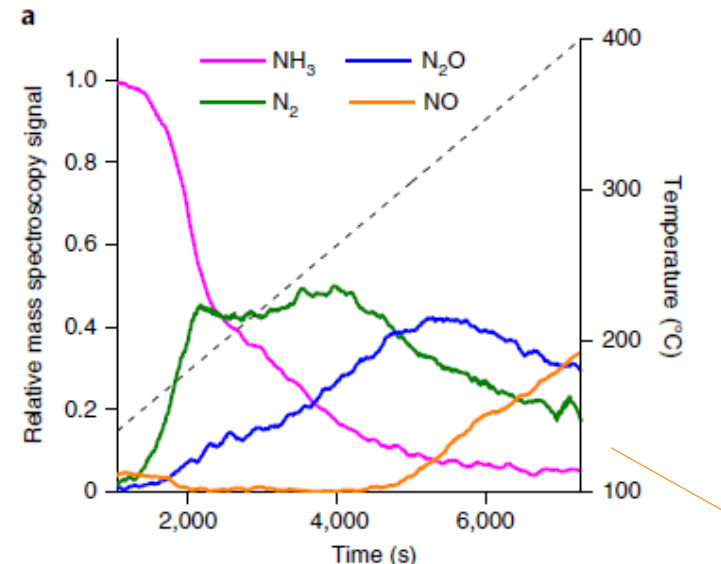


Bond	Bond length (Å)			
	From EXAFS		From XRD	
	Crystallized state			
Ge-Te	$2.83 \pm 0.01$		$3.0(1) \pm 0.3$	
Sb-Te	$2.91 \pm 0.01$		$3.0(1) \pm 0.3$	
Te-Te (2nd)	$4.26 \pm 0.01$		$4.2(6) \pm 0.2$	
	Laser-amorphized state			
Ge-Te	$2.61 \pm 0.01$		2.61*	
Sb-Te	$2.85 \pm 0.01$			

Enormous difference in the precision comparing EXAFS with XRD

Spectra measured at the K-edges of: Ge, Sb and Te. On amorphization the bonds become shorter (as shown by shifts in the peak positions) and stronger, that is, more locally ordered (as shown by increase in the peak amplitudes and decrease in the peak widths).

## EXAFS on Pd nanoparticles for catalytic NH<sub>3</sub> oxidation



Pd particles are a catalyst used to transform the ammonia (NH<sub>3</sub>) in the exhaust gas of cars via:

$$NH_3 + O_2 -> N_2 + H_2O$$

Without formation of NO

NO formation after some exposure due to Pd-N formation

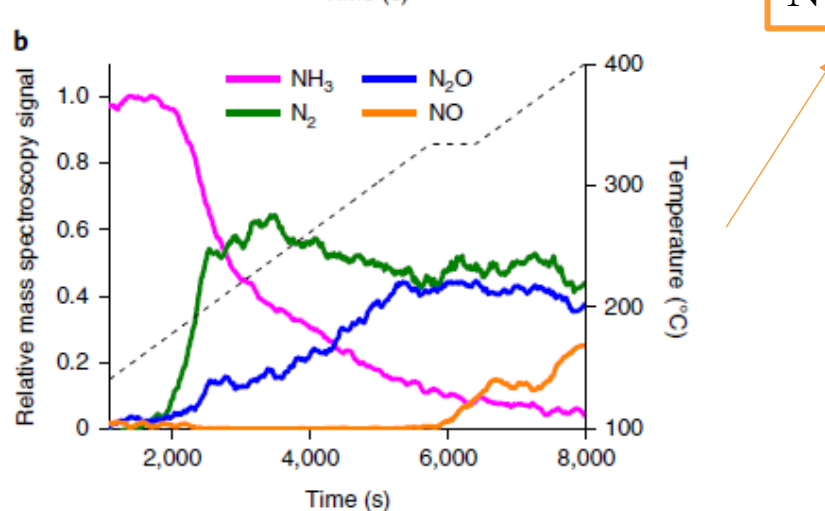
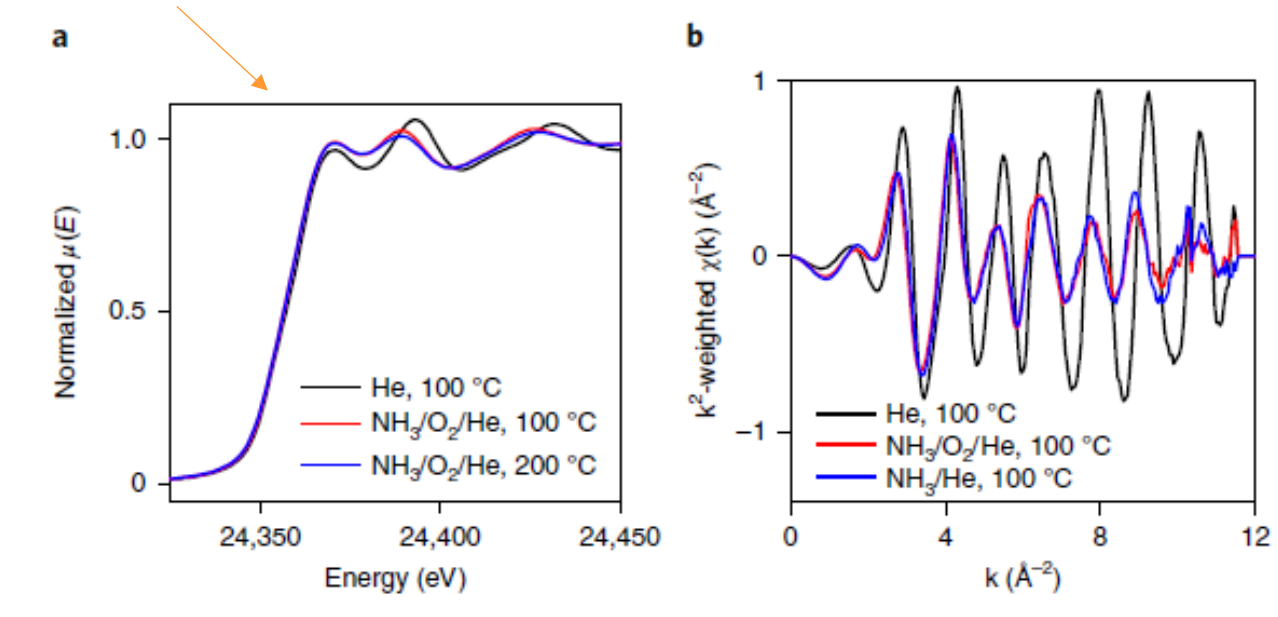


Fig. 1 | Catalytic activity of supported Pd catalysts for NH $_3$  oxidation at increasing temperatures. a, 1.5 wt% Pd/zeolite-Y. b, 1.5 wt% Pd/ $\gamma$ -Al $_2$ O $_3$ . Reactant gas feed: 0.5% NH $_3$ ; 2.5% O $_2$ ; 97% He. Dashed line, catalyst temperature.



EXAFS at the Pd K-edge shows disruption of the local atomic order due to Pd-N formation